REPORT No. 765

EXHAUST-STACK NOZZLE AREA AND SHAPE FOR INDIVIDUAL CYLINDER EXHAUST-GAS JET-PROPULSION SYSTEM

By Benjamin Pinkel, L. Richard Turner, Fred Voss, and Leroy V. Humble

SUMMARY

An investigation was conducted on the effect of exhaust-stack nozzle area, shape, and length on engine power, jet thrust, and gain in net thrust (engine propeller plus jet). Single-cylinder engine data were obtained using three straight stacks 25, 44, and 108 inches in length; an S-shaped stack, a 90° bend, a 180° bend, and a short straight stack having a closed branch faired into it. Each stack was fitted with nozzles varying in exit area from 0.91 square inch to the unrestricted area of the stack of 4.20 square inches. The engine was generally operated over a range of engine speeds from 1300 to 2100 rpm, inlet-manifold pressures from 22 to 36 inches of mercury absolute, exhaust pressures from 12 to 30 inches of mercury absolute, and a fuel-air ratio of 0.08.

The loss in engine power, the jet thrust, and the gain in net thrust are correlated in terms of several simple parameters. An example is given for determining the optimum nozzle area and the over-all net thrust.

INTRODUCTION

In 1932 it was shown by computations in reference 1 that an appreciable increase in net thrust horsepower (engine propeller plus jet) might be expected on an aircraft engine when the exhaust stack of each engine cylinder is directed to discharge rearwardly. Flight data of the XP–41 airplane in 1940 (reference 2) showed that net thrust gains of the magnitude predicted by computations could be obtained in practice.

In the flight investigation on the XP–41 airplane, two exhaust-stack nozzle sizes (exit areas) were tried and it was found that the smaller nozzles gave larger jet thrust than the larger nozzles but, because the smaller nozzles introduced too great a restriction to the exhaust-gas flow, a loss in engine power occurred with the result that the net thrust horsepower and the maximum airplane velocity were greater for the larger nozzles. The maximum net thrust horsepower would probably have been obtained with an intermediate nozzle size. This investigation indicated the need for data to determine the optimum exhaust nozzle size for maximum net thrust horsepower. Consequently an investigation was conducted at the NACA Langley Field laboratory during 1940–41, using a straight exhaust stack 25 inches long with various nozzle exit areas. This investigation was reported in reference 3.

A second investigation was conducted in 1942 using exhaust stacks of various shapes such as would be necessary for aircraft installations. Four different shapes and two additional lengths were tested with various nozzle exit areas. This investigation was reported in reference 4.

Reported herein is a summary of references 3 and 4 giving the effect of exhaust-nozzle area, stack shape, and length, on engine power, jet thrust, and the gain in over-all net thrust in terms of several simple parameters. An example is given for the design of optimum jet stacks and for the gain in net thrust horsepower.

SYMBOLS

A	nozzle area, (sq ft)
F	mean exhaust-gas thrust, (lb)
f	fuel-air ratio
I	indicated power, (hp)
I_o	indicated power with unrestricted exhaust stack, (hp)
M_e	average mass flow of exhaust gas, (slugs/sec)
n	engine speed, (rps)
p_o	atmospheric pressure, (lb/sq ft or in. Hg absolute)
p_m	inlet-manifold pressure, (lb/sq ft or in. Hg absolute)
R	gas constant of air, (ft-lb)/(slug) (°F)
T_m	inlet-manifold temperature, (°R)
v_d	displacement volume, (cu ft)
V	airplane velocity, (ft/sec)
$\overline{V}_e$	mean exhaust-gas jet velocity, (ft/sec)
$(\overline{V}_e)_{eff}$	effective mean exhaust-gas jet velocity, (ft/sec)
η_p	propeller efficiency
η_v	volumetric efficiency of engine
$\eta_{v.o}$	volumetric efficiency with unrestricted exhaust stack

$$\phi = \frac{550\ I}{p_m v_d \frac{n}{2}} = \frac{imep}{p_m}$$

$$\phi_o = \frac{550\ I_o}{p_m v_d \frac{n}{2}}$$

$$\Delta\phi = \phi - \phi_o$$

$$\Delta\eta_v = \eta_v - \eta_{v.o}$$

ANALYSIS

The gas in the cylinder at the end of the expansion stroke is at a pressure considerably above atmospheric and is capable of performing an appreciable amount of work by further expansion. Jet propulsion provides a means for utilizing this work. The potential energy in the cylinder is transformed into kinetic energy in the exhaust jet and the thrust is derived from jet reaction.

In the conventional aircraft engine the gases are discharged through the valve passage with acoustic velocity and considerable loss in the availability of the energy occurs because of acoustic shock and because the kinetic energy is transformed into heat by turbulence and friction in the bends and changes in passage area and shape. These losses can be reduced by providing nozzles at the end of the exhaust stacks. The use of nozzles having small areas as compared with the valve-passage area will obviously reduce flow losses because then the velocity through the valve passages and exhaust ports would be small with the result that the shock, friction, and turbulence losses would be decreased. The pressure would be transferred from the cylinder to the nozzle, where it may be efficiently converted into velocity. Operation with extremely small nozzles, however, would result in the trapping of high-pressure exhaust gas in the engine cylinder and would cause a considerable loss in engine power. The optimum nozzle area is defined as that area which provides the maximum sum of the thrust powers of the engine and of the jet.

The indicated horsepower is defined as the difference in horsepowers of the power process (compression and expansion strokes) and of the discharging and charging processes and is assumed to be proportional to the charge-air flow. It is further assumed that during the charging process the residual gas in the clearance volume is compressed adiabatically to the inlet-manifold pressure p_m. Based on this definition and these assumptions reference 3 shows that the ratio ϕ of *imep* to p_m is mainly a function of p_o/p_m and $v_d n/A$ for constant T_m, f, and spark advance. The change in engine power resulting from the restriction of the exhaust-stack exit area is represented by the quantity $\Delta\phi$ and

$$\Delta\phi=\phi-\phi_o=f_1\left(\frac{p_e}{p_m},\frac{v_d n}{A}\right) \tag{1}$$

Similarly volumetric efficiency η_v and change in volumetric efficiency due to restriction of the exhaust stack $\Delta\eta_v$ can be shown to be functions of p_o/p_m and $v_d n/A$.

By assuming that the largest part of the exhaust gas is discharged from the nozzle with acoustic velocity, reference 3 shows that the mean exhaust-gas jet velocity $\overline{V}_e$ is a function principally of $p_o A/M_e$. Thus

$$\overline{V}_e=\frac{F}{M_e}=f_2\left(\frac{p_o A}{M_e}\right) \tag{2}$$

The net thrust horsepower when exhaust-gas jet thrust is utilized is the sum of engine-propeller-thrust and jet-thrust horsepowers. In reference 4 it has been shown that the change in net thrust horsepower is proportional to

$$\Delta\phi_T=\Delta\phi+\frac{(1+f)}{RT_m}\eta_v\overline{V}_e\frac{V}{\eta_p} \tag{3}$$

In order to account for a change in drag caused by any changes in the quantity of engine charge air, the term $-\Delta\eta_v\frac{V^2}{RT_m\eta_p}$ should be added to the right side of equation (3). Because it is impractical to operate with a nozzle area restricted to such an extent as to affect the volumetric efficiency, this term has been dropped. The above equation is based on the assumption that the change in brake horsepower caused by nozzle restriction at constant engine speed is the same as the change in indicated power. The quantity $\Delta\phi_T$ is considered as a net increase in the mean effective pressure of the engine divided by the inlet-manifold pressure. If $\Delta\phi_T$ is considered to be due to an effective mean exhaust-gas jet velocity $(\overline{V}_e)_{eff}$, it may be expressed as

$$\Delta\phi_T=\frac{(1+f)}{RT_m}\eta_v\frac{V}{\eta_p}(\overline{V}_e)_{eff} \tag{4}$$

The substitution of equation (3) into equation (4) and the solution for $(\overline{V}_e)_{eff}$ gives

$$(\overline{V}_e)_{eff}=\frac{RT_m}{(1+f)\eta_v}\frac{\eta_p}{V}\Delta\phi+\overline{V}_e \tag{5}$$

It has previously been shown that $\Delta\phi$ and η_v are functions mainly of p_o/p_m and $v_d n/A$ and that $\overline{V}_e$ is a function of $p_c A/M_e$, but

$$\frac{p_o A}{M_e}=\frac{p_o}{p_m}\frac{A}{v_d n}\frac{2RT_m}{(1+f)\eta_v} \tag{6}$$

Thus, if p_o/p_m is constant, $\Delta\phi$ and η_v may be considered functions of $p_o A/M_e$ and for constant V/η_p, it is seen that $(\overline{V}_e)_{eff}$ is also a function of $p_o A/M_e$.

APPARATUS

Exhaust-gas stacks and nozzles.—Several differently shaped exhaust stacks were used. These stacks included (a) three straight stacks 25, 44, and 108 inches in length, (b) an offset or S-shaped stack, (c) a 90° bend, (d) a 180° bend, and (e) a straight stack having a closed branch faired into it. The length of the curved stacks varied from 11¼ inches for the 90° bend to 44 inches for the 180° bend. The length of all the stacks included the length of the nozzle. Each stack had an inside diameter of 2⅝ inches. A sketch giving the main dimensions of the curved stacks is shown in figure 1. In some cases it was convenient to use short inserts in the stack as an aid in changing nozzles. These inserts are shown by dashed lines in figure 1.

The nozzles used with each of the stacks were 5 inches long and consisted of a 3-inch tapered section faired into 1-inch straight sections at each end. The nozzle-exit areas ranged from 0.91 to 4.20 (unrestricted stack) square inches.

Setup.—The single-cylinder test engine for this investigation was an 1820–G engine modified to operate with only

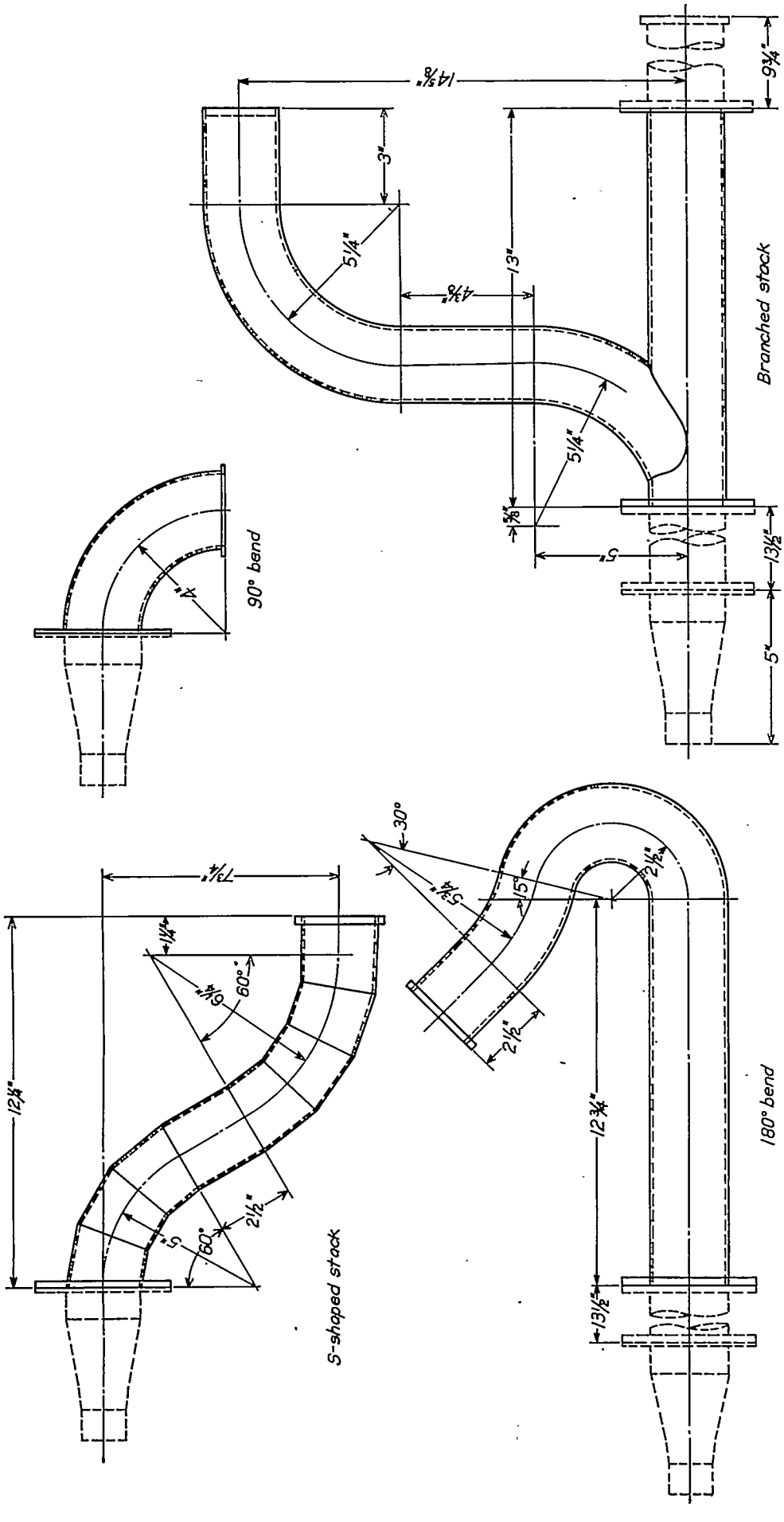

FIGURE 1.—Exhaust-stack shapes. (All stacks are 2 9/16-in. inside diam.)

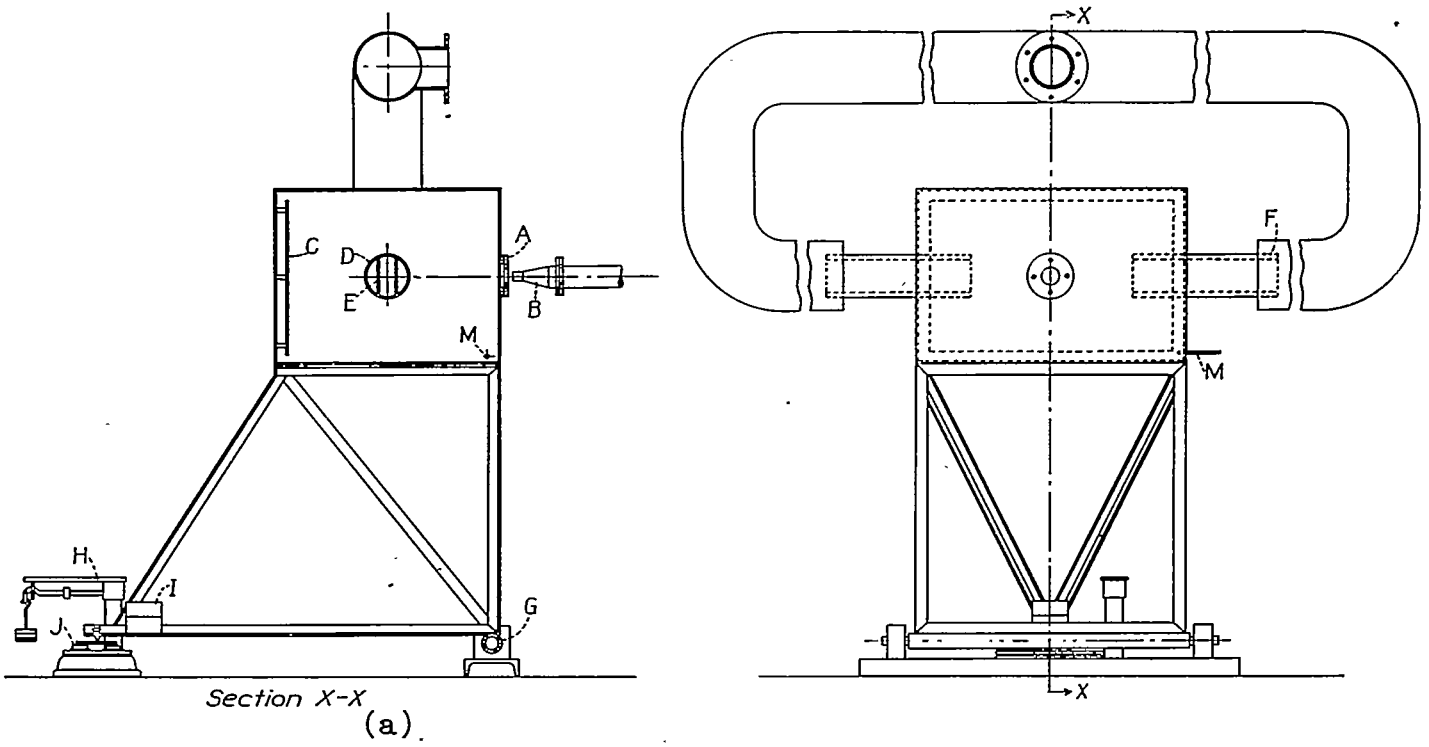

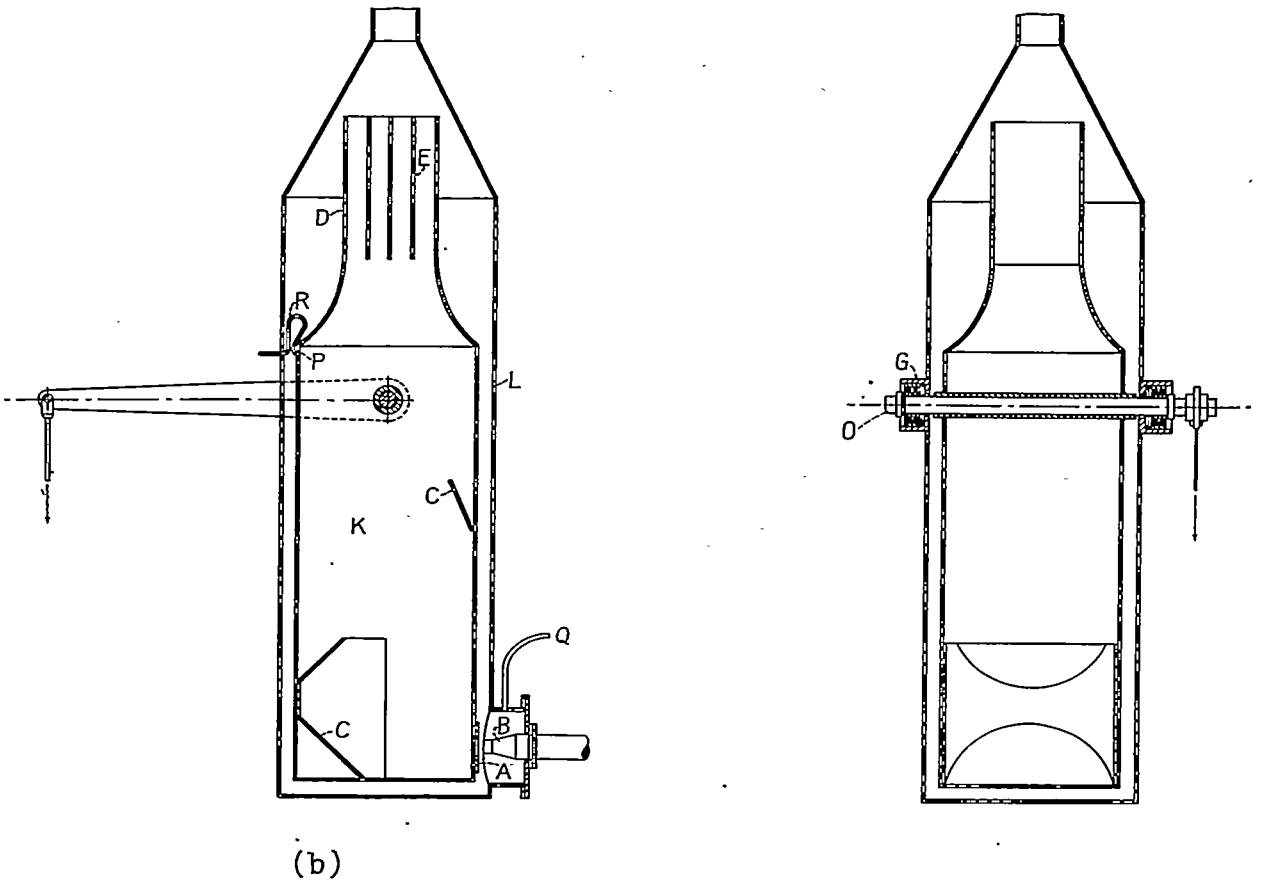

(a) Target for sea-level exhaust pressure.
(b) Target for altitude exhaust pressure.

FIGURE 2.—Diagram of thrust-measuring device.

one cylinder. The regular crankcase, crankshaft, cams, piston, and master connecting rod were retained. The compression ratio was 6.4. The air-cooled cylinder was enclosed in a sheet-metal jacket open at the front and the rear; a motor-driven centrifugal blower provided the necessary cooling air. Air for the supercharged condition was obtained from the laboratory central air supply. An electric dynamometer was used to measure the torque of the engine and an electrically operated revolution counter and a stop watch were used to determine the engine speed. Thermocouples were provided to measure cylinder temperatures. The engine charge air was measured by means of an orifice plate in the air-intake duct. A tank was installed between the engine and the orifice plate to damp out pulsations. The fuel flow was measured by a calibrated rotameter.

The tank into which the exhaust gas was discharged during the tests to determine the effect of exhaust-nozzle restriction and stack shape on engine power with various exhaust pressures had a volume of approximately 70 cubic feet. The engine exhaust stack was connected to the tank with a length of flexible tubing. A tap for measuring static pressure was located in the tank. Tank pressures were maintained by operation of an exhauster.

The mean exhaust-gas thrust at sea-level exhaust pressure was measured by means of the thrust target shown diagrammatically in figure 2 (a). The exhaust gas discharged from the nozzle B, entered the target through the hole in the cover plate A, impinged on the stainless-steel plate C, and left the target through the two pipes D normal to the jet and parallel to the axis of support of the target. These pipes were provided with vertical guide vanes E to insure discharge of the gas from the tank in a direction normal to the nozzle axis. The exhaust manifold F fitted over these pipes but without contact. The hole in the cover plate A was approximately ⅜ inch greater in diameter than the nozzle-exit passage. A different plate was used for each nozzle size. The end of the nozzle was located approximately ¼ inch from the plate A. Pressure tap M was located in the target in a position to measure only static pressure. This target was used only with the 25-inch stack and the various nozzles.

Exhaust-gas thrust measurements at simulated altitude conditions were made by means of the thrust target shown in figure 2 (b). The target K was suspended within the tank L, which was connected to an exhauster. Altitude pressures could be maintained in the tank by operation of the exhauster. The nozzle B was attached to the tank L in a manner to prevent leakage. The exhaust gas entered the target through the hole in the cover plate A. As in the previous case, a separate cover plate was provided for each nozzle. Deflectors C were provided to distribute the exhaust gas in the target and guide vanes E, to insure discharge of the exhaust gas through the exit pipe D in a direction perpendicular to the nozzle exit. The axis of the pipe D intersected the axis of the hollow shaft O in order to minimize torsional reaction to the discharge of exhaust gas from the target. Water was circulated through the hollow shaft O for cooling. Static-pressure taps P and Q were located in the target and the tank, respectively. The pressure was transmitted from tap P through a thin tube R coiled to provide a negligible restraining force on the target. The pressures were measured by means of manometers.

Both of the targets were supported on ball bearings G. The exhaust thrust was determined from readings of the platform scale H (fig. 2 (a)) and the moment arms. In order to overcome vibration, the load on the scales was increased by weights I and carried on rubber bushings J.

Army 100 octane fuel was used in this investigation.

METHODS

EFFECT OF NOZZLE AREA AND STACK SHAPE ON ENGINE POWER

The effect of exhaust-stack nozzle area and stack shape on engine power was determined at engine speeds of 1300, 1500, 1700, 1900, and 2100 rpm and at maximum power fuel-air ratio, 0.08. Variation in speed of ± 10 rpm and in fuel-air ratio of ± 0.002 was permitted. In general, for each exhaust nozzle and stack shape, the engine was operated at each speed over the following range of conditions:

(a) Constant inlet-manifold pressure at 30 inches mercury absolute and variable exhaust-tank pressures from 12 to 30 inches mercury absolute.

(b) Variable inlet-manifold pressures from 24 to 30 inches of mercury absolute and constant exhaust-tank pressure at 30 inches mercury absolute.

In addition, variable manifold-pressure runs up to 36 inches mercury absolute were made for the 25-inch stack.

The 108-inch stack with several nozzle areas was investigated at engine speeds from 1300 to 2100 rpm in steps of approximately 100 rpm and at constant ratios p_o/p_m of 0.4, 0.7, and 1.0.

In all runs the oil-out temperature was held between 140° and 160° F and the cooling-air pressure drop was held at approximately 20 inches of water. The carburetor-air temperature remained at approximately 80° F, with a maximum variation of ± 10° F. The engine power and charge-air consumption were corrected to a carburetor-air temperature of 80° F on the assumption that they vary inversely as the square root of the absolute temperature. Motoring friction with the unrestricted 25-inch exhaust stack was measured at each speed with sea-level inlet and exhaust pressures. These values were plotted against engine speed and the data were faired.

The indicated mean effective pressure for all stack shapes and nozzles were calculated by adding to the brake mean effective pressure, the friction mean effective pressure determined from the faired friction curve. The ratio of the indicated mean effective pressure to the inlet-manifold pressure ϕ was plotted against the ratio of exhaust-tank pressure to inlet-manifold pressure p_o/p_m.

The volumetric efficiency η_v was calculated from the weight of charge air by means of the following relation:

$$\eta_v = \frac{2RT_m}{v_d n p_m} \times \text{mass of charge air per second}$$

The volumetric efficiency was plotted against p_o/p_m.

The quantity $\Delta\phi$ for each nozzle and stack was taken as the difference between the value of ϕ for the nozzle and for the unrestricted exhaust stack at the same values of engine speed and p_o/p_m. The values of $\Delta\phi$ were calculated from the faired curves of ϕ and plotted against $v_d n/A$ for constant values of p_o/p_m as suggested by equation (1) in the analysis. The quantity $\Delta\eta_v$ was determined in a manner similar to that described for $\Delta\phi$.

EFFECT OF NOZZLE AREA AND STACK SHAPE ON EXHAUST-GAS THRUST

The thrust of the exhaust gas was determined by discharging the exhaust gas into the targets shown in figure 2 and by reading on the scale a quantity proportional to the reaction of the target. Because each target was designed to discharge the exhaust gas at right angles to the direction that it issued from the exhaust stack, the reaction of the target is equal to the exhaust-gas thrust. The target reaction was calculated from the scale reading by multiplying by the lever-arm ratio.

The thrust determinations were made with the 25-inch stack, the 180° bend, and the branched stack. Each stack was tested at engine speeds of 1300, 1500, 1700, 1900, and 2100 rpm with several different nozzle areas. In general, for each nozzle area the engine was operated over the following range of conditions:

(a) Constant inlet-manifold pressure at 30 inches of mercury absolute and variable thrust-target pressures from 12 to 30 inches of mercury absolute.

(b) Variable inlet-manifold pressures from 24 to 30 inches of mercury absolute and constant thrust-target pressure at 30 inches of mercury absolute.

In some cases for the 25-inch stack, the inlet-manifold pressure was varied from 22 to 36 inches mercury absolute

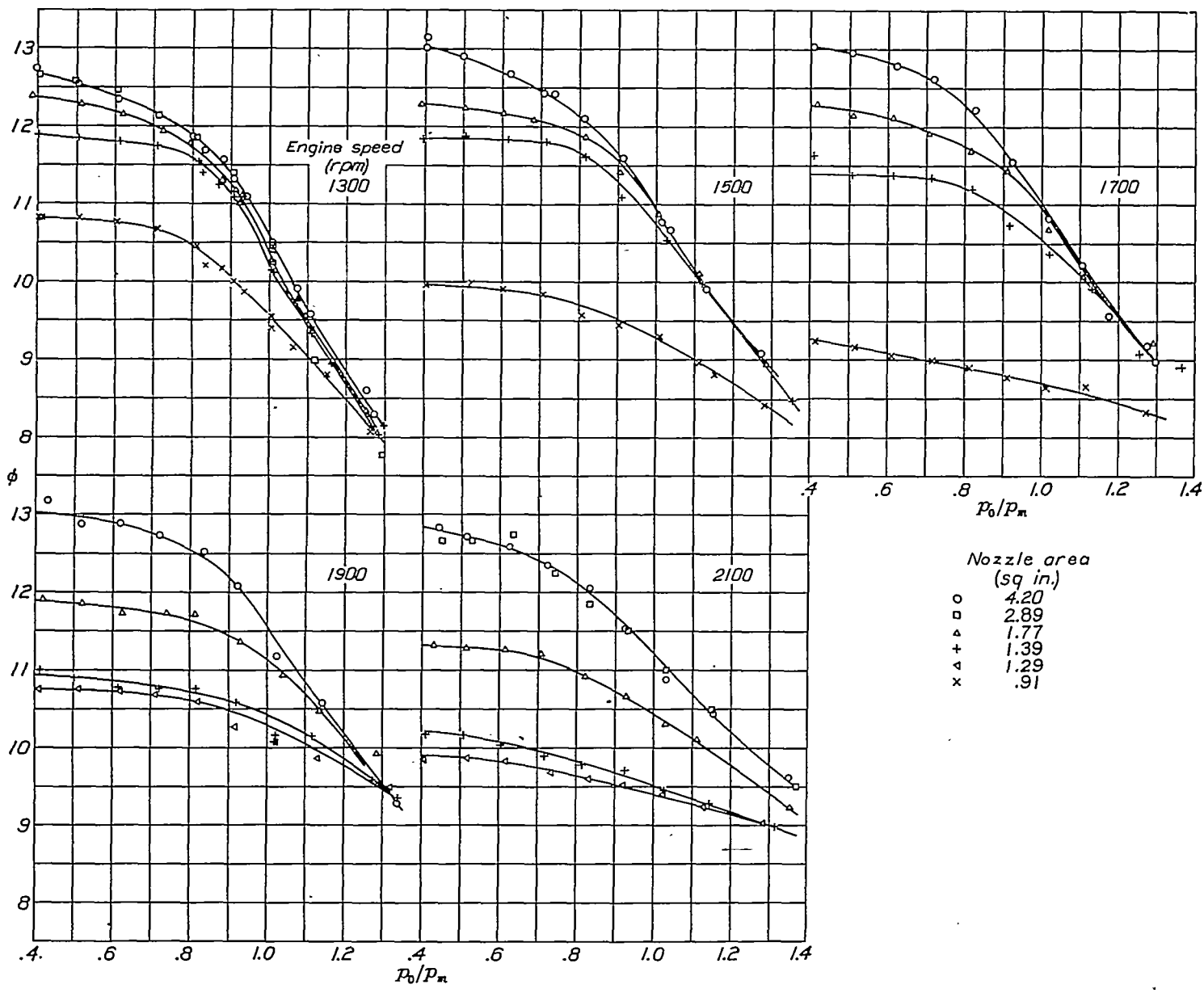

FIGURE 3.—Variation of ϕ with p_o/p_m and nozzle area at constant engine speeds for 25-inch stack.

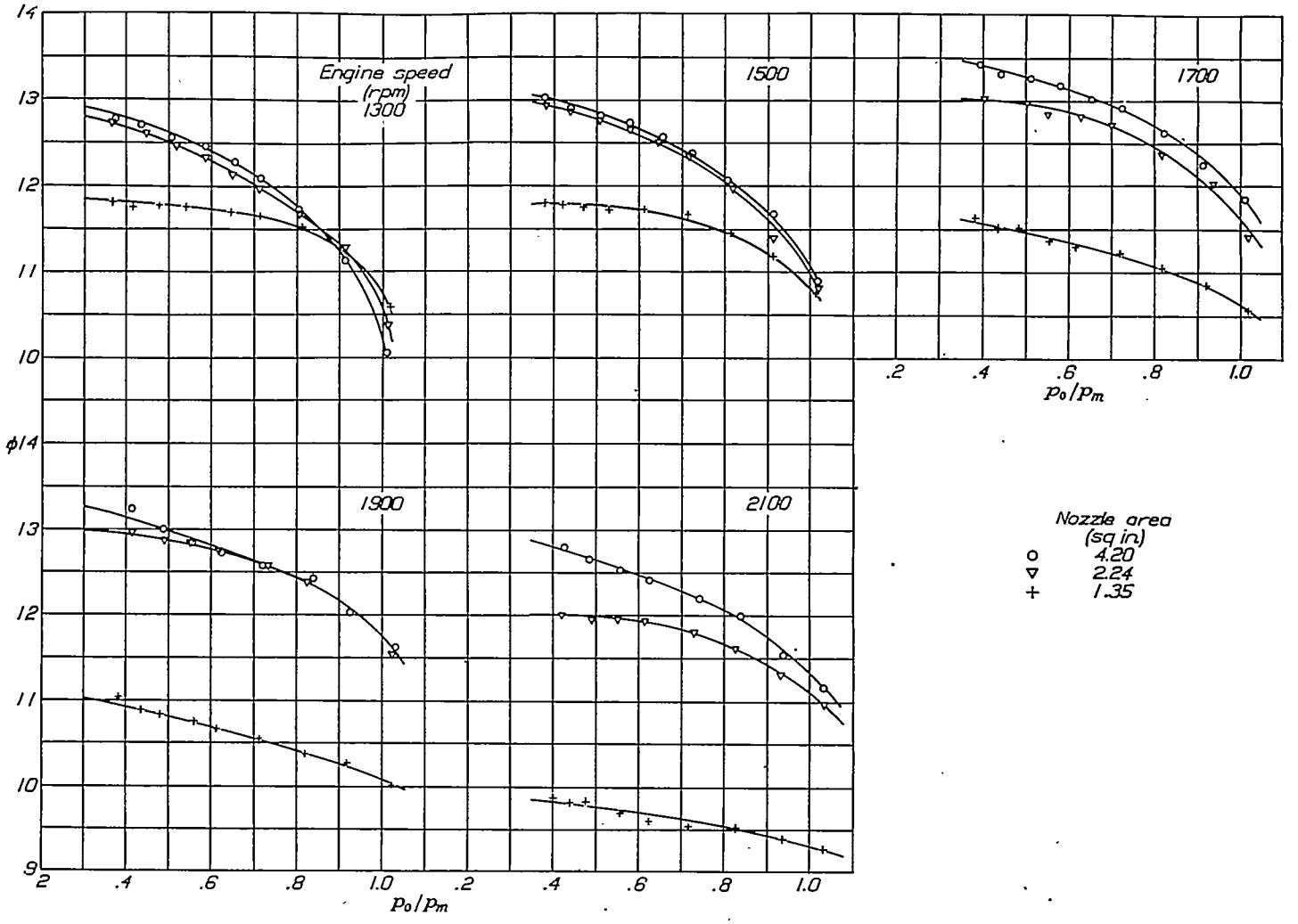

FIGURE 4.—Variation of ϕ with p_o/p_m and nozzle area at constant engine speeds for 44-inch stack.

with the thrust-target pressure constant at 30 inches of mercury absolute.

The weight of exhaust gas was determined by means of the calibrated orifice in the air-intake duct and the rotameter in the fuel line. The thrust data are presented by plotting the ratio F/M_e or $\overline{V}_e$ against p_oA/M_e in accordance with equation (2) in the analysis.

For the purpose of checking the exhaust thrust measurements and studying the exhaust process, indicator cards were taken in the cylinder and in the 25-inch exhaust stack by means of a Farnboro pressure indicator at an engine speed of 1900 rpm and sea-level inlet-manifold and exhaust pressure for six nozzle areas from 0.91 to 4.20 square inches. The impact pressure in the exhaust stack and the instantaneous and the average thrust were calculated from the indicator cards by the method given in appendix II of reference 3.

DISCUSSION OF RESULTS

THE EFFECT OF NOZZLE AREA AND STACK SHAPE ON ENGINE POWER

The variation of the ratio ϕ of *imep* to the inlet-manifold pressure with the ratio of atmospheric to inlet-manifold pressure p_o/p_m for a range of nozzle areas and engine speeds is shown in figure 3 for the 25-inch stack. The curves marked 4.20-square-inch nozzle area on this and subsequent figures represent the unrestricted exhaust-stack condition. The same curve was obtained for a given nozzle and engine speed regardless of which term in the quantity p_o/p_m was varied. This result is in agreement with the analysis. Generally, ϕ for constant engine speed and nozzle area decreases at an increasing rate as p_o/p_m increases. The value of ϕ at constant engine speed and p_o/p_m and the average rate of decrease of ϕ with p_o/p_m decrease with a decrease in nozzle area.

The variation of ϕ with p_o/p_m for the 44-inch stack is shown in figure 4. Comparison with the data for the 25-inch stack (fig. 3) shows that no appreciable change was caused by the increased length. However, when the length was increased to 108 inches, the effects of resonance between the natural frequency of pressure waves in the exhaust system and engine speed were appreciable and no correlation was obtained by plotting ϕ against p_o/p_m. The long stack was found to have an adverse effect on engine power for most practical combinations of engine speed and nozzle area. (See fig. 20, reference 4.)

The variation of ϕ with p_o/p_m for the 90° bend, the S-shaped stack, the 180° bend, and the branched stack are shown in figures 5, 6, 7, and 8, respectively. These curves have the same general shape as those for the 25-inch stack

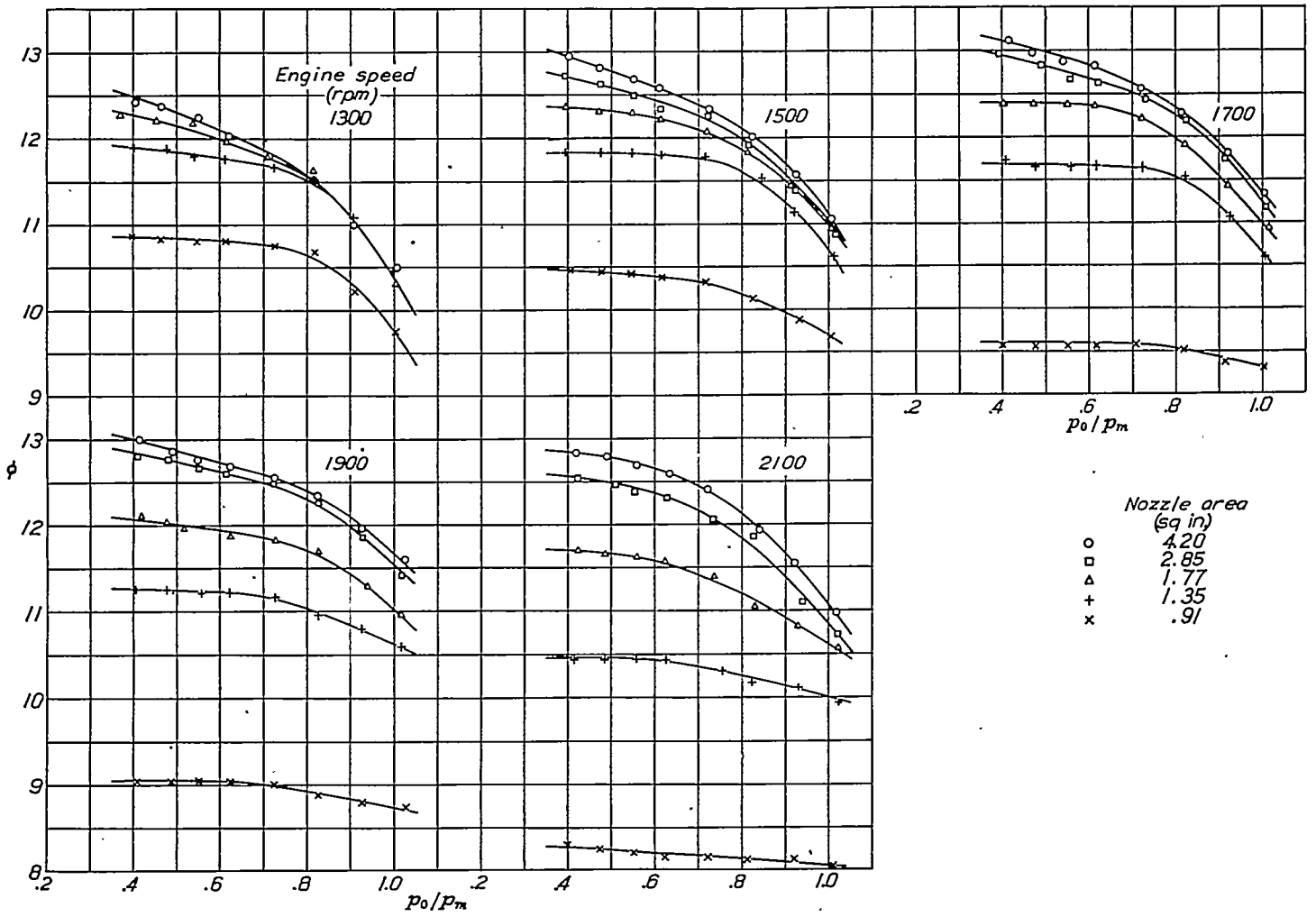

FIGURE 5.—Variation of ϕ with p_0/p_m and nozzle area at constant engine speeds for 90° bend.

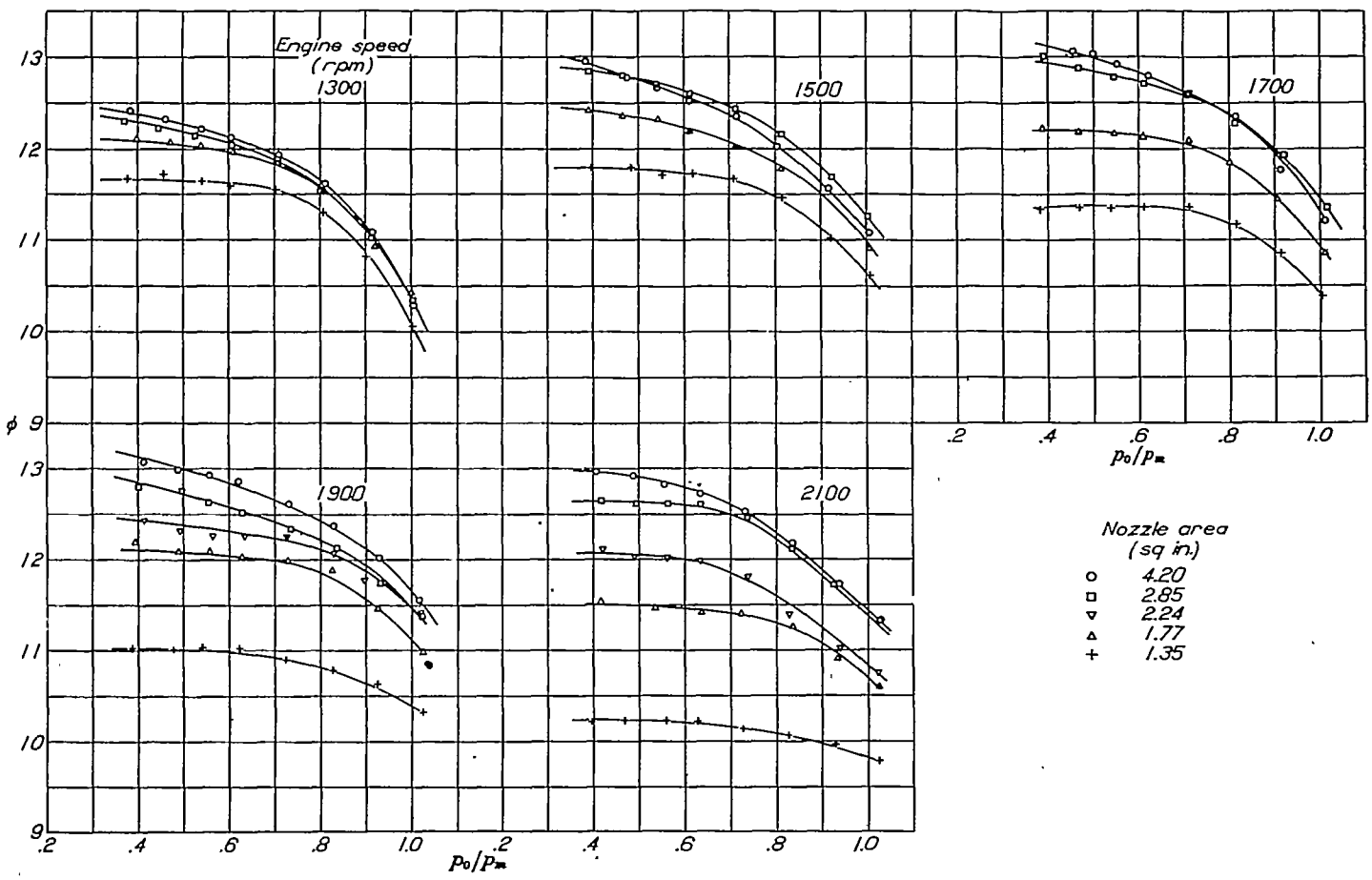

FIGURE 6.—Variation of ϕ with p_0/p_m and nozzle area at constant engine speeds for S-shaped stack.

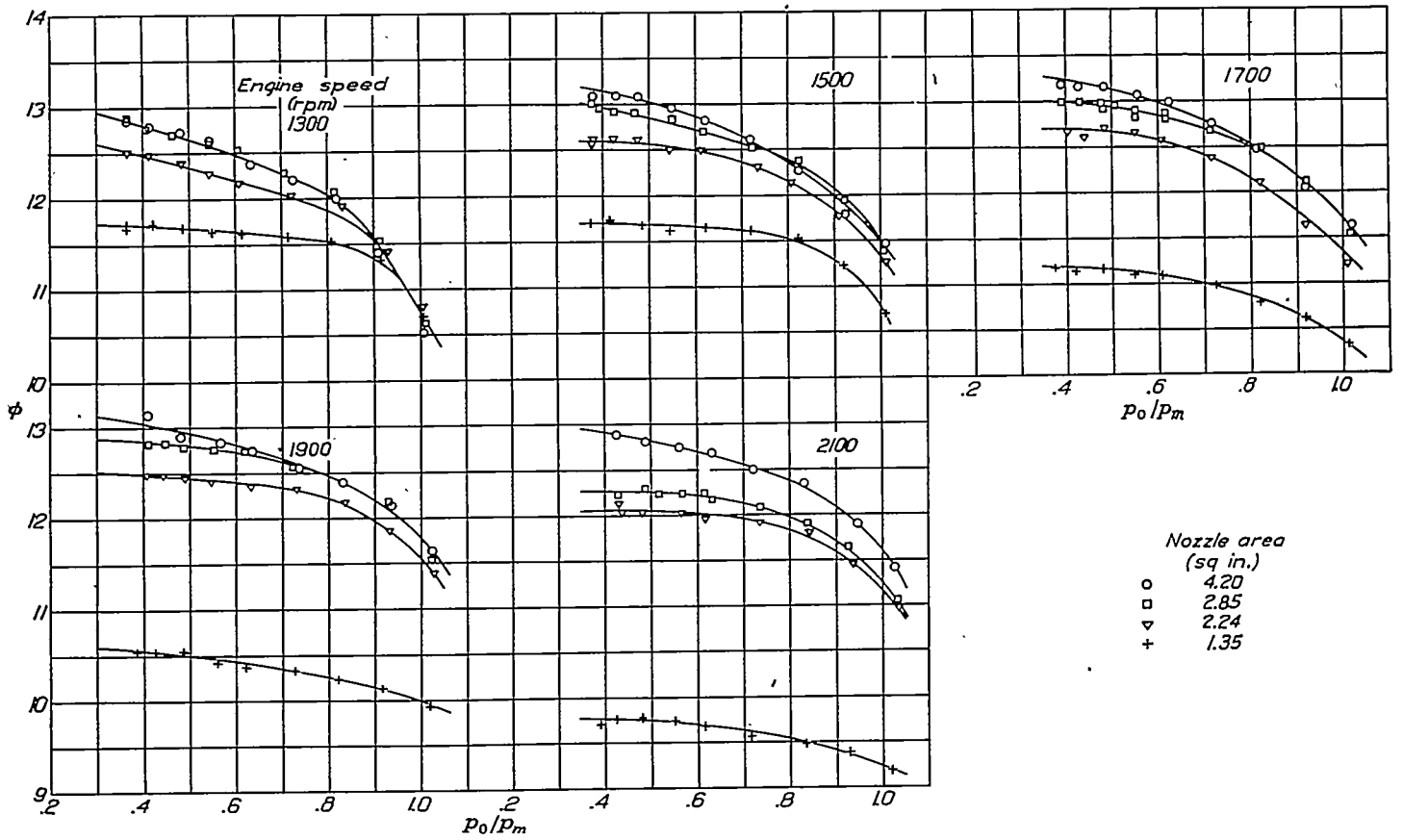

FIGURE 7.—Variation of ϕ with p_0/p_m and nozzle area at constant engine speeds for 180° bend.

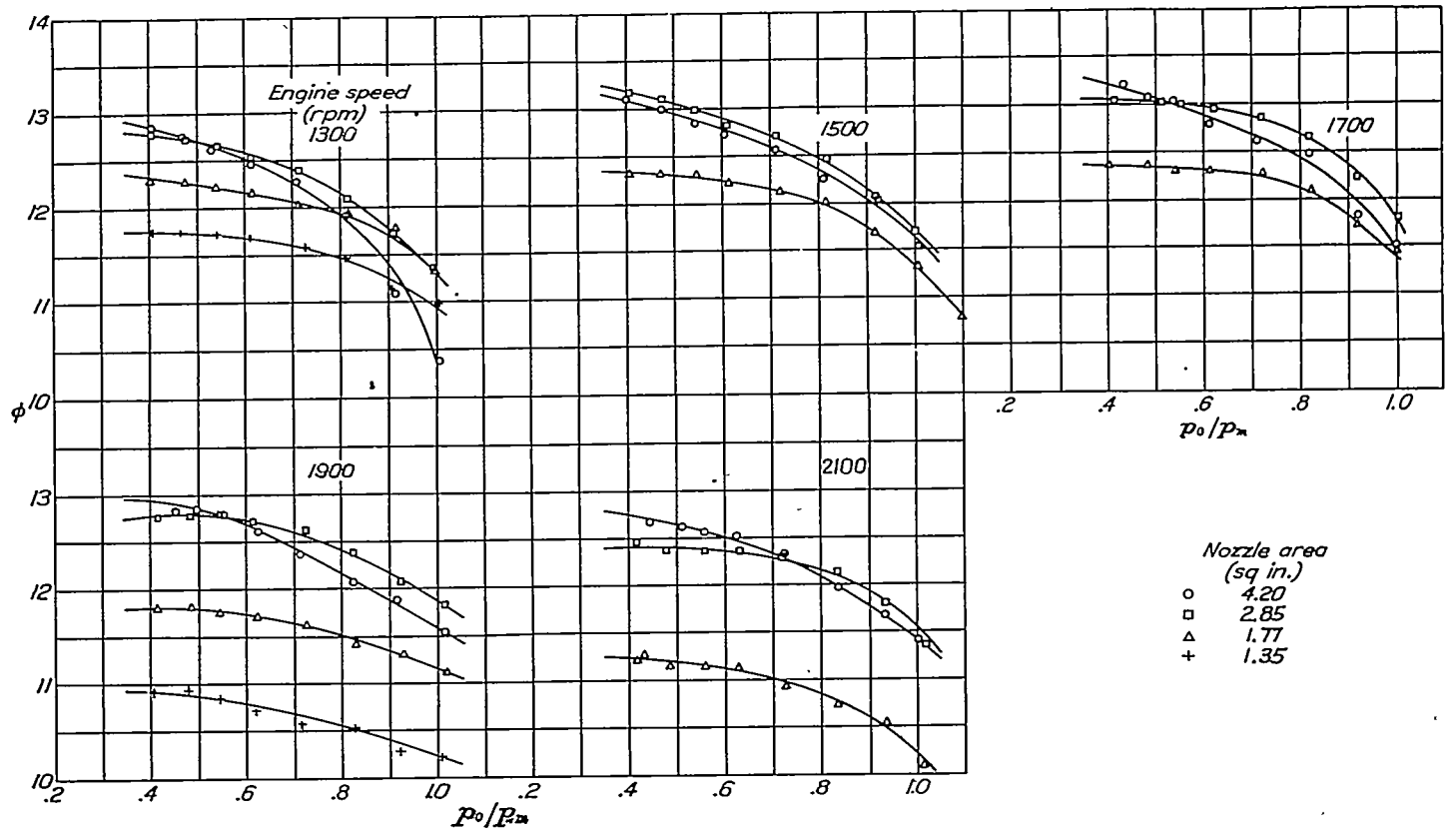

FIGURE 8.—Variation of ϕ with p_0/p_m and nozzle area at constant engine speeds for branched stack.

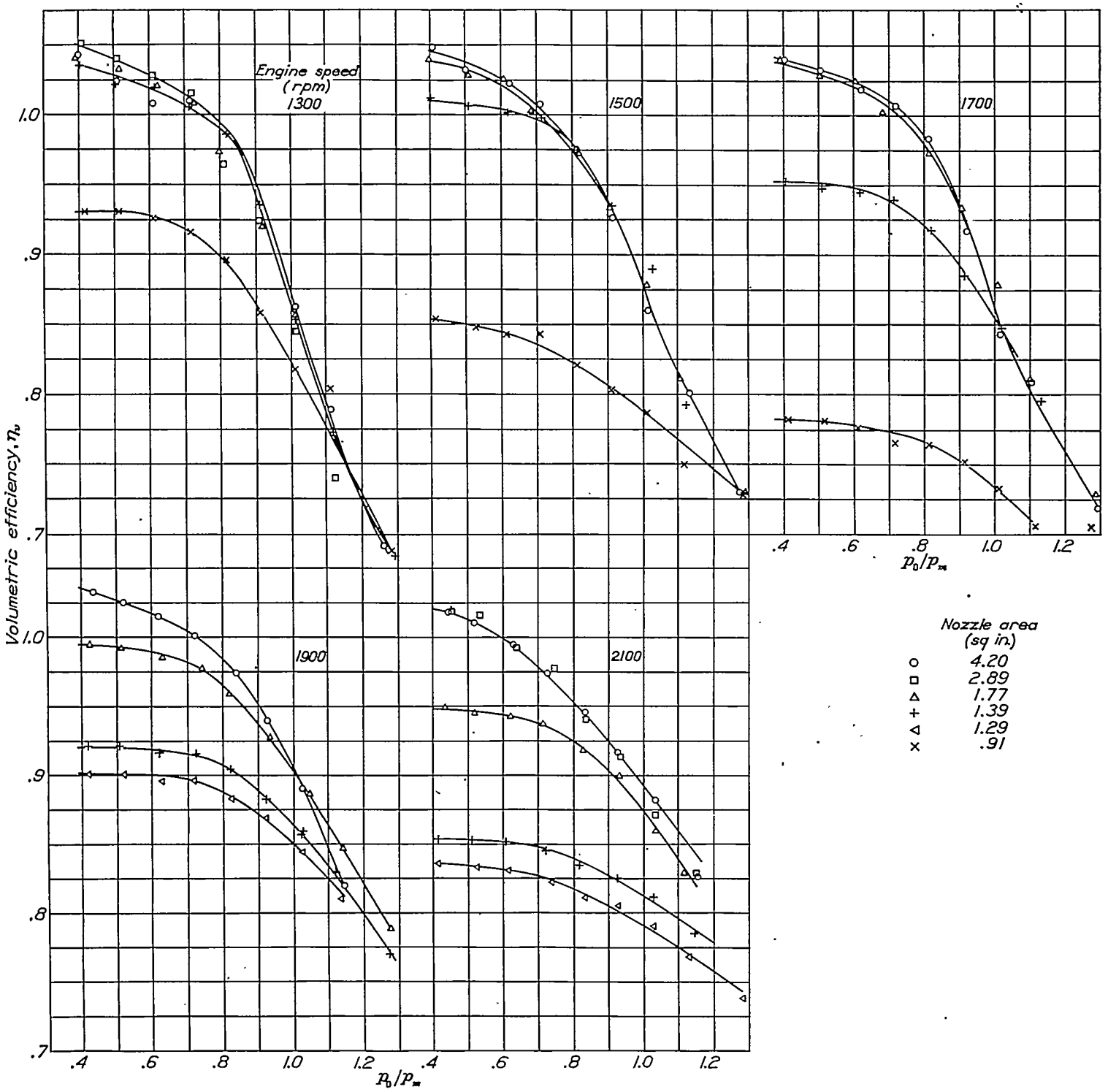

FIGURE 9.—Variation of volumetric efficiency η_v with p_0/p_m and nozzle area at constant engine speeds for 25-inch stack.

(fig. 3). The variation of ϕ with p_o/p_m for these stacks with unrestricted nozzles agrees fairly well with that for the 25-inch stack.

The variation of volumetric efficiency η_v with p_o/p_m for constant engine speeds and nozzle areas is shown in figures 9 and 10 for the 25-inch stack and the S-shaped stack, other stacks, which will be presented later, were obtained by extrapolating the curves of ϕ against p_o/p_m. It is noted that a single curve is obtained when $\Delta\phi$ is plotted against $v_d n/A$ regardless of whether engine speed or nozzle size is varied further substantiating the analysis. At low values of $v_d n/A$, $\Delta\phi=0$ but as $v_d n/A$ increases a point is reached

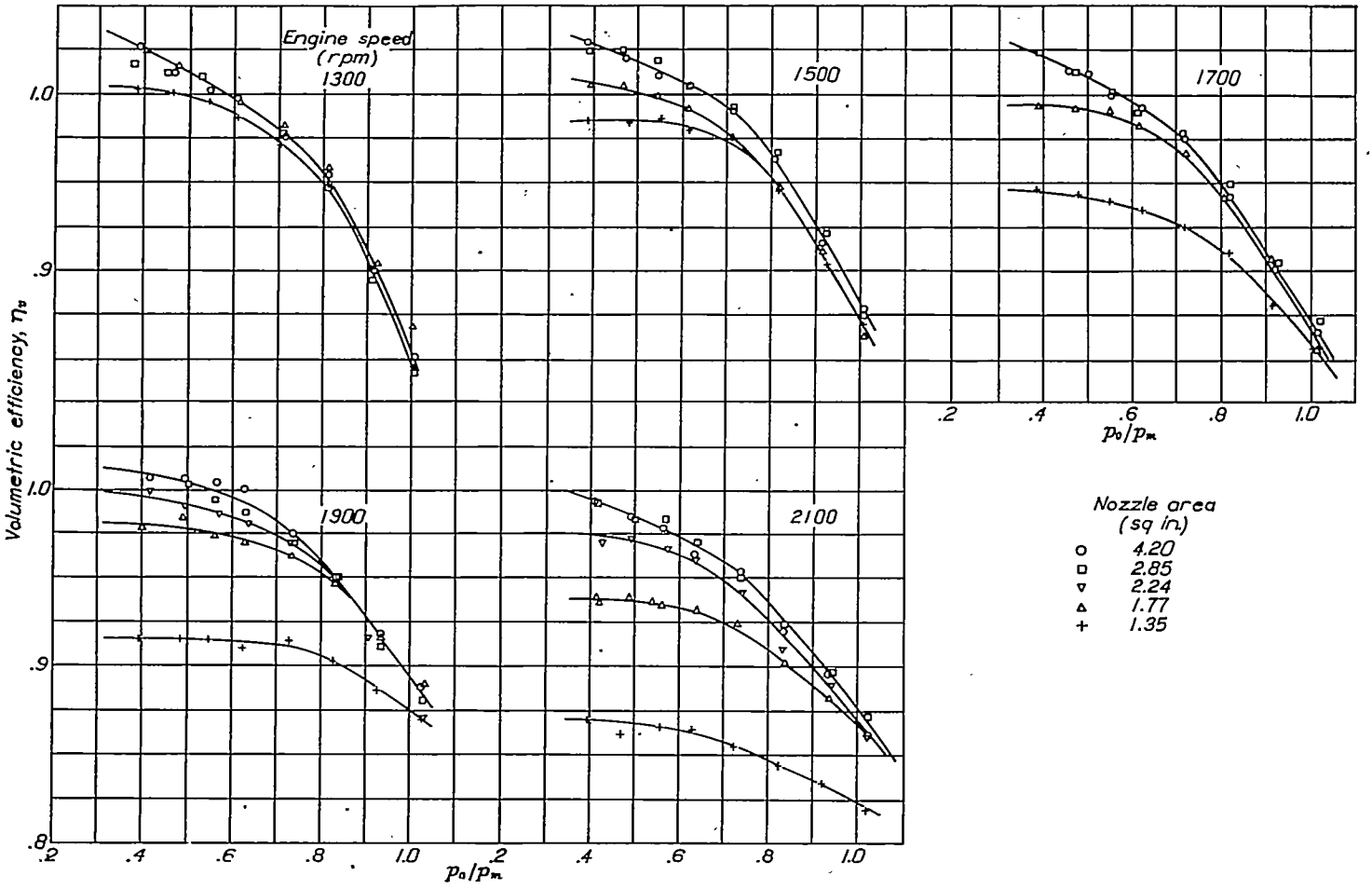

FIGURE 10.—Variation of volumetric efficiency η_v with p_o/p_m and nozzle area at constant engine speeds for S-shaped stack.

respectively. These results are typical of the other stacks and have the same general shape as the ϕ curves.

The change in engine power caused by exhaust-nozzle restriction for constant engine speed and p_o/p_m is represented by $\Delta\phi$. Because the value of ϕ for the unrestricted area is subtracted from that for the restricted area, negative values of $\Delta\phi$ indicate a loss in engine power.

The values of $\Delta\phi$ for the 25-inch stack are shown in figure 11 plotted against $v_d n/A$ for various values of p_o/p_m. The values of $\Delta\phi$ at $p_o/p_m=0.2$ for this stack as well as those for where $\Delta\phi$ decreases sharply with further increase in $v_d n/A$. Although a smooth transition from the region $\Delta\phi=0$ to the region of loss in power $\Delta\phi<0$ probably occurs, the transition is sufficiently abrupt that no appreciable error results from drawing separate straight lines through the points in the two regions. The intersections of these lines mark the critical values of $v_d n/A$ or the values at which the engine begins to lose power. The curves of $\Delta\phi$ for the 44-inch stack and the branched stack (not presented) show a similar sharp transition.

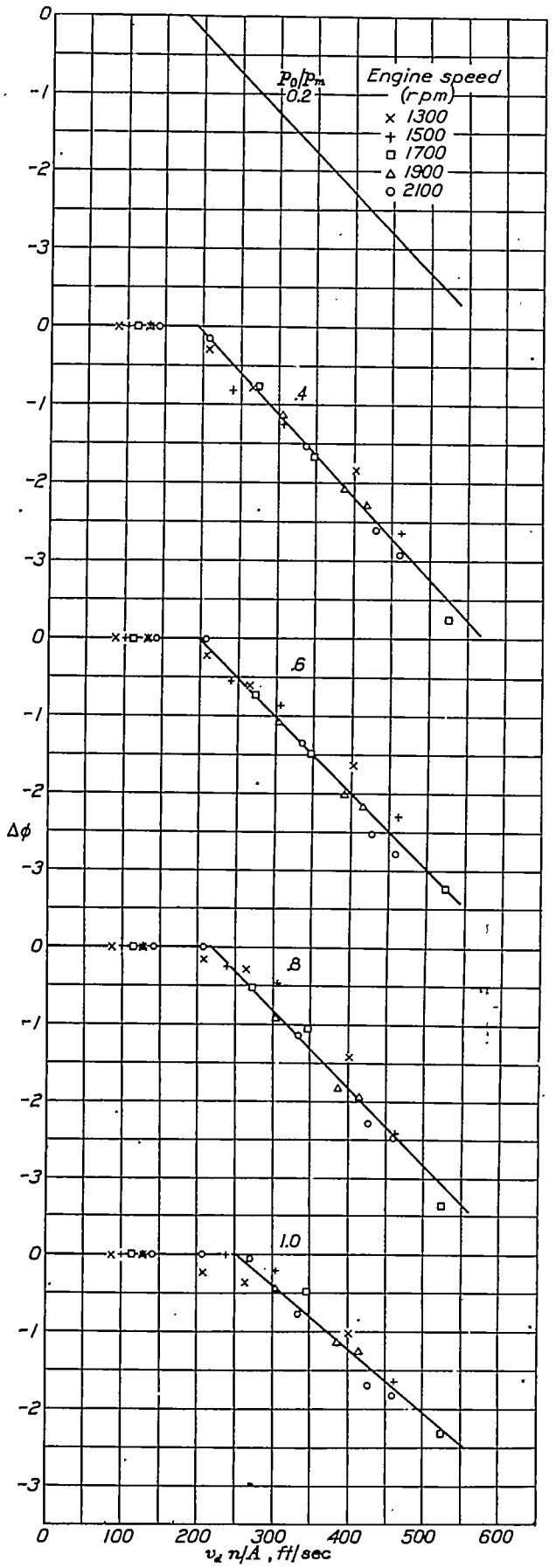

FIGURE 11.—Variation of $\Delta\phi$ with $v_d n/A$ for 25-inch stack.

Values of $\Delta\phi$ are plotted against $v_d n/A$ in figures 12 and 13 for the 90° bend and the S-shaped stacks, respectively. There appears to be a smooth transition from the region of no loss in power to the region where a loss occurs. The values of $\Delta\phi$ for 180° bend (not presented) show a similar smooth transition. Thus it appears that curved stacks have a smooth transition in contrast to straight stacks up to 44-inches long with or without a branch. Comparison of figures 11, 12, and 13 shows that the rate of decrease of engine power with decrease of nozzle area for the curved stacks is initially less than that for the 25-inch stack, but approaches the rate for the 25-inch stack as nozzle area is greatly reduced.

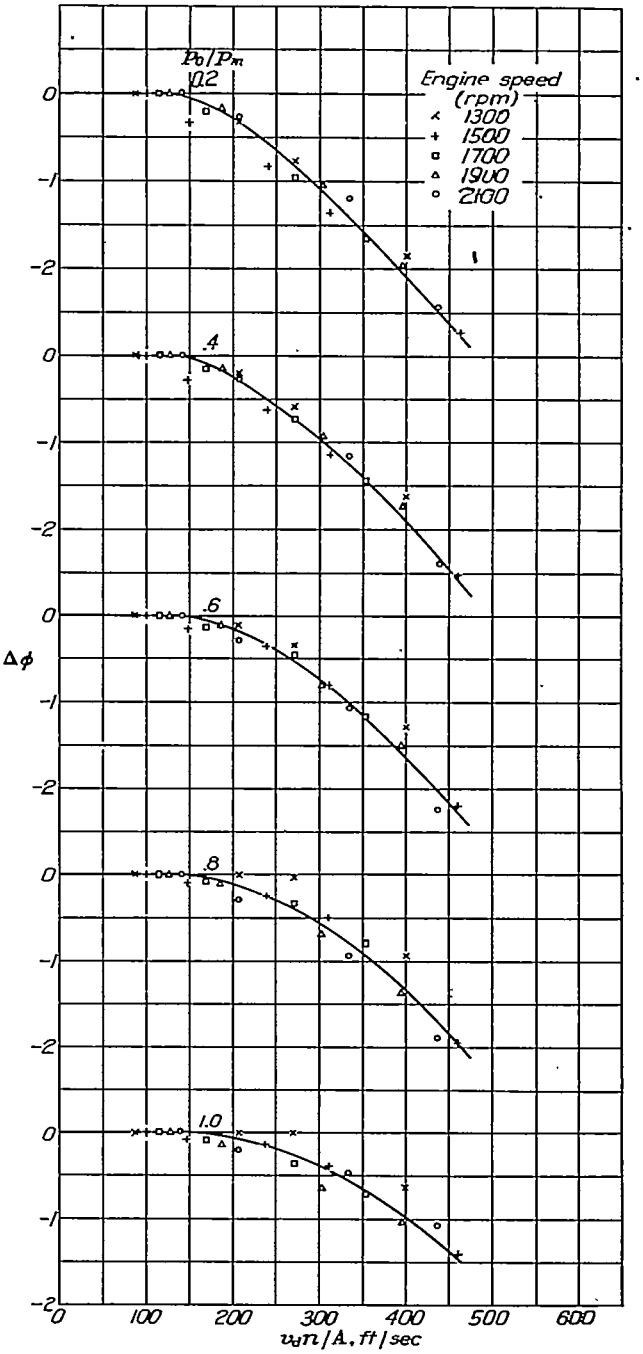

FIGURE 12.—Variation of $\Delta\phi$ with $v_d n/A$ for 90° bend.

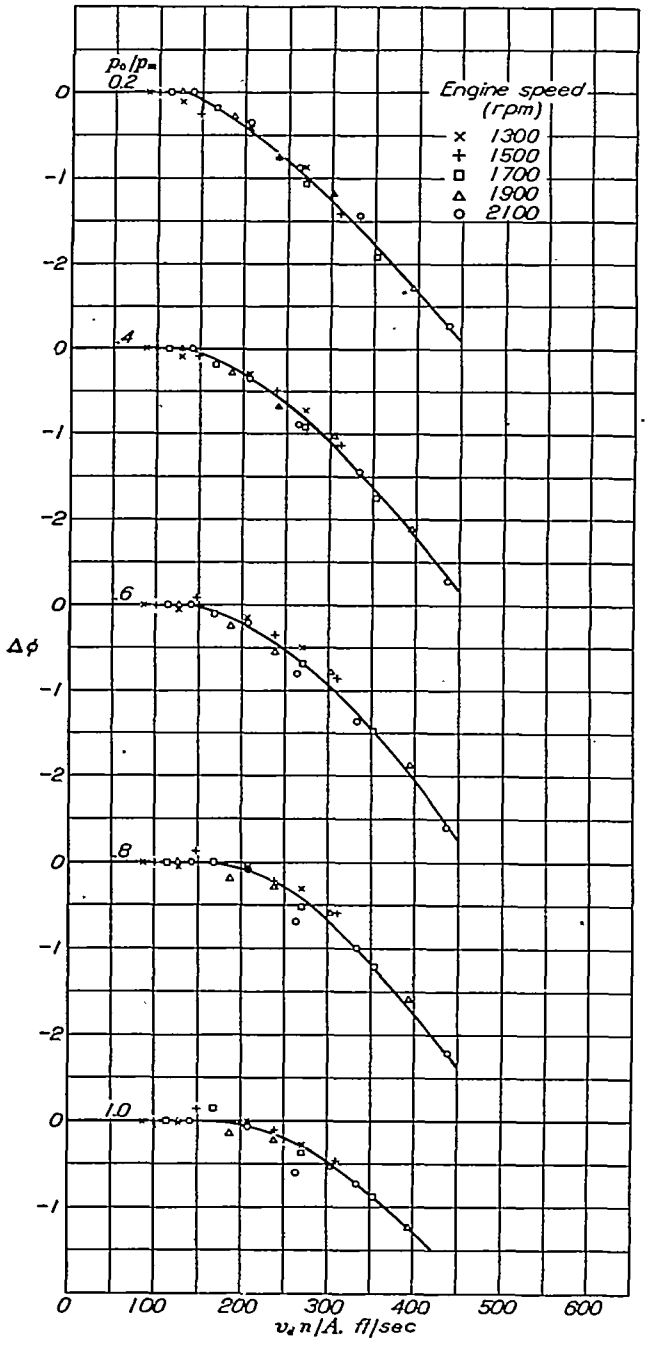

FIGURE 13.—Variation of $\Delta\phi$ with $v_d n/A$ for S-shaped stack.

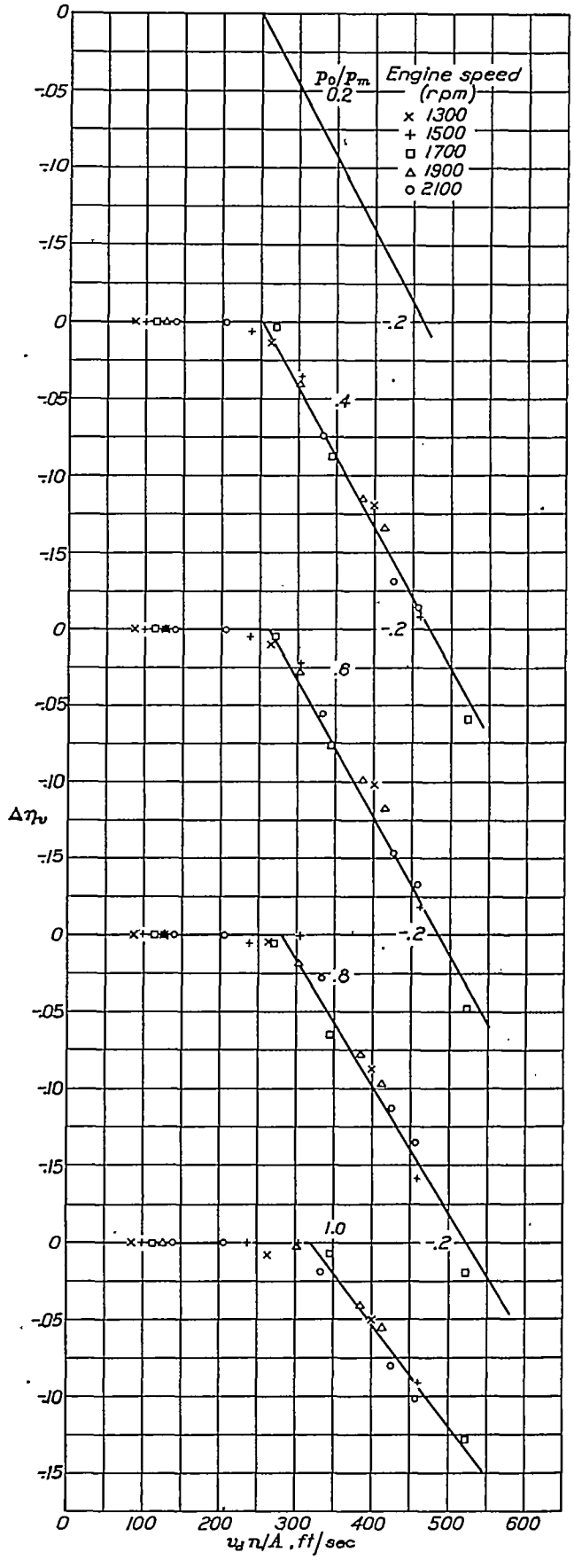

FIGURE 14.—Variation of $\Delta\eta_v$ with $v_d n/A$ for 25-inch stack.

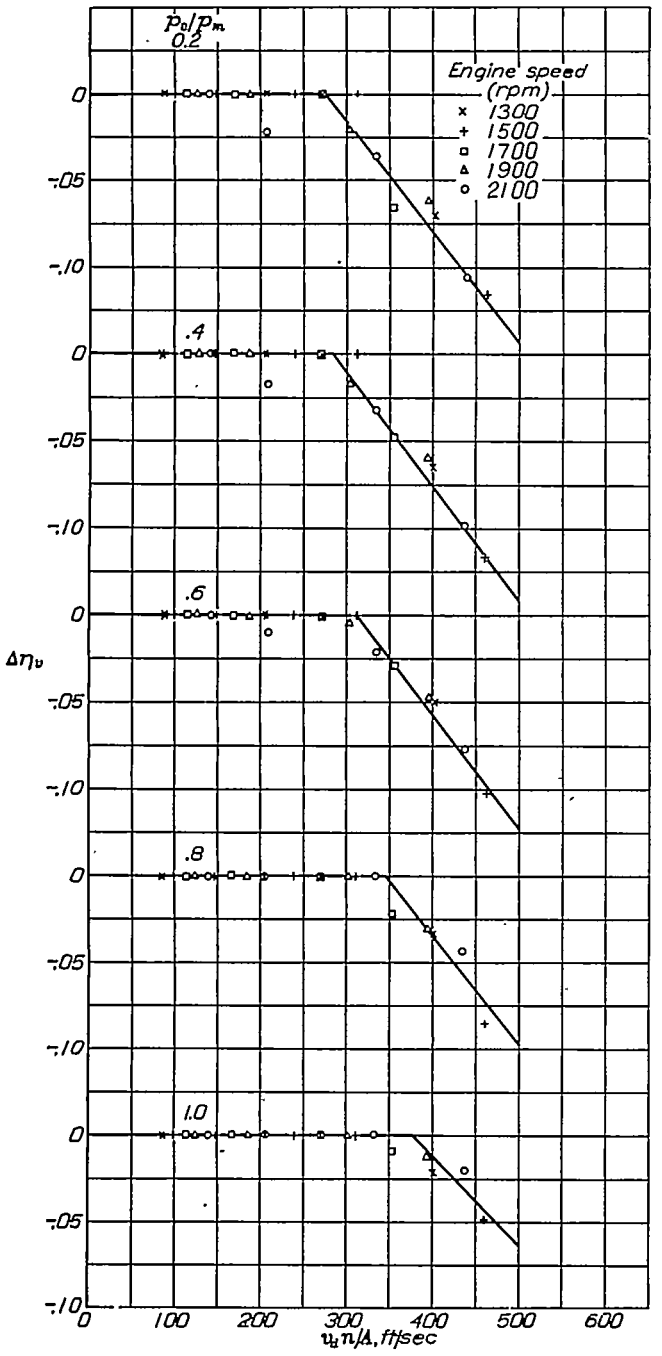

FIGURE 15.—Variation of $\Delta\eta_v$ with $v_d n/A$ for 90° bend.

The values of $\Delta\eta_v$ for the 25-inch, the 90° bend, and the S-shaped stacks are shown in figures 14, 15, and 16, respectively, plotted against $v_d n/A$ for various values of p_o/p_m. The values of $\Delta\eta_v$ at $p_o/p_m=0.2$ were obtained by extrapolating the η_v curves. These curves and those for the other shapes not presented show some scatter and two straight intersecting lines represent the data as well as any curve. A smaller nozzle can be used with the 90° bend without loss in volumetric efficiency than for the 25-inch or S-shaped stack.

A comparison of the $\Delta\phi$ and the $\Delta\eta_v$ curves shows, as the nozzle area is reduced for a given set of operating conditions, that the point at which power loss begins is reached before the engine loses volumetric efficiency. The difference is caused by the increase in piston work with the reduction in nozzle size, which becomes noticeable before the loss in volumetric efficiency.

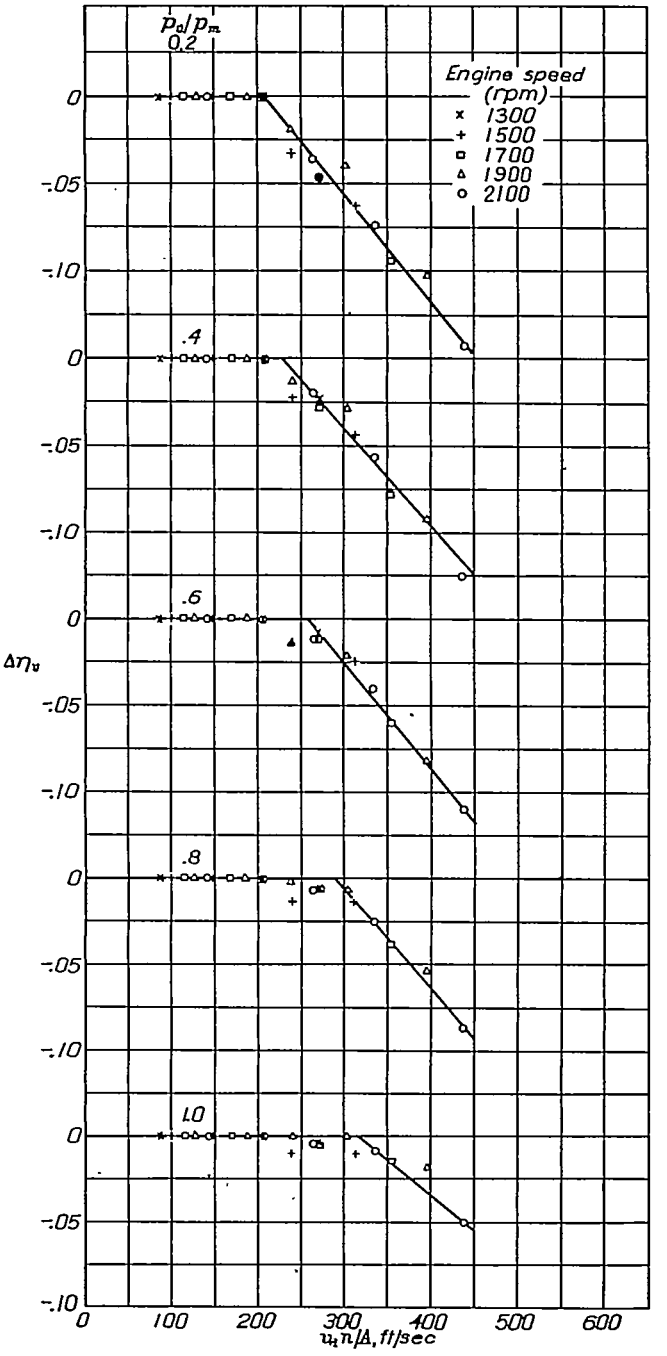

FIGURE 16.—Variation of $\Delta\eta_v$ with $v_d n/A$ for S-shaped stack.

The critical values of $v_d n/A$, or values at which the engine just begins to lose power ($\Delta\phi=0$), are shown in figure 17 for all the stacks. For all the stacks the critical value of $v_d n/A$ increases with p_o/p_m. The curves for the 25-inch stack are superimposed on each curve of the other stacks for ready comparison. The critical values for the 44-inch stack agree with those for the 25-inch stack over the range of p_o/p_m. The branched stack has lower values for low values of p_o/p_m but agrees with those for the 25-inch stack at values of p_o/p_m above 0.7. The values for the three curved stacks are about 60 feet per second lower than those for the 25-inch stack over the range of p_o/p_m.

EFFECT OF NOZZLE SIZE AND STACK SHAPE ON EXHAUST THRUST

The data on the effect of nozzle size on exhaust-gas thrust for the 25-inch stack are shown in figures 18 and 19, in which the thrust as represented by $\overline{V}_e$ is plotted against $p_o A/M_e$. All the data are plotted as a single curve in figure 18. The points for each nozzle area are plotted on separate curves in figure 19 and are keyed according to engine speed and to inlet and exhaust conditions in order to allow examination of the data for any trend with these variables. The curves in figure 19 are sections of the curve faired through all of the data (fig. 18).

The dispersion of the points in figure 19 appears to be mainly the result of experimental error as no trend can be noticed with the separate variables. It may be concluded from an examination of this figure that plotting $\overline{V}_e$ against $p_o A/M_e$ provides a good correlation of the data over the complete range of operating conditions.

The variation of $\overline{V}_e$ with $p_o A/M_e$ for the exhaust stack having a 180° bend is shown in figure 20 (a). Inspection of the figure shows that the data agree satisfactorily with the curve obtained for the 25-inch stack. Because the exhaust-gas thrust obtained with the 180° bend agreed with that obtained with the 25-inch stack and as stacks having bends of less than 180° may be expected to have correspondingly less effect on exhaust-gas thrust, it is believed that the curve of $\overline{V}_e$ against $p_o A/M_e$ for the 25-inch stack may be used to predict the thrust obtainable with all single stacks having smooth bends of various degrees.

The variation of $\overline{V}_e$ with $p_o A/M_e$ for the branched stack is plotted in figure 20 (b). The data with the unrestricted stack fit the curve for the 25-inch stack fairly well, but those with the restricted nozzles are somewhat smaller for a given value of $p_o A/M_e$. This difference is probably due to the increase in stack volume caused by the presence of the branch; the added volume acts to reduce the pressure of the gas in the stack and thereby increases the throttling losses at the exhaust valve and hence reduces the mean jet velocity.

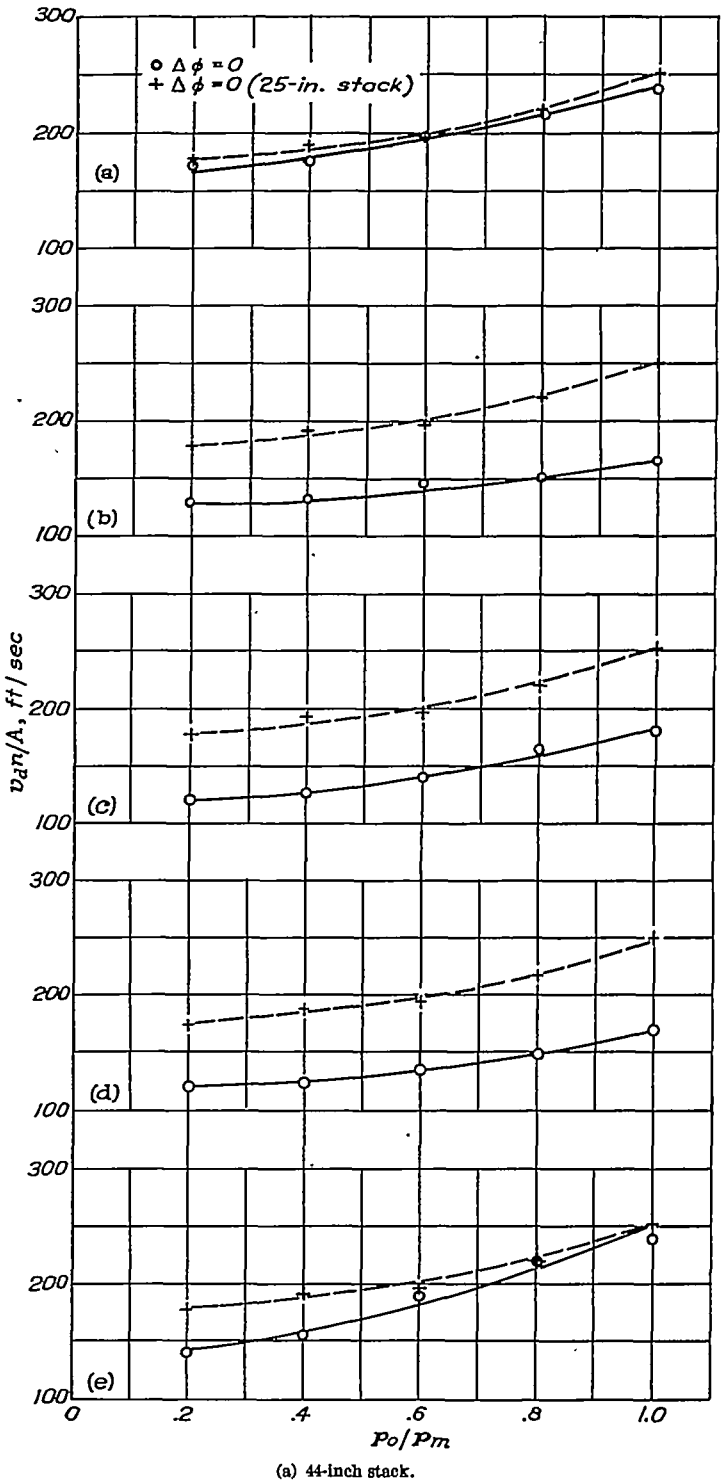

(a) 44-inch stack.
(b) 90° bend.
(c) S-shaped stack.
(d) 180° bend.
(e) Branched stack.

FIGURE 17.—Variation of critical values of $v_d n/A$ with p_o/p_m.

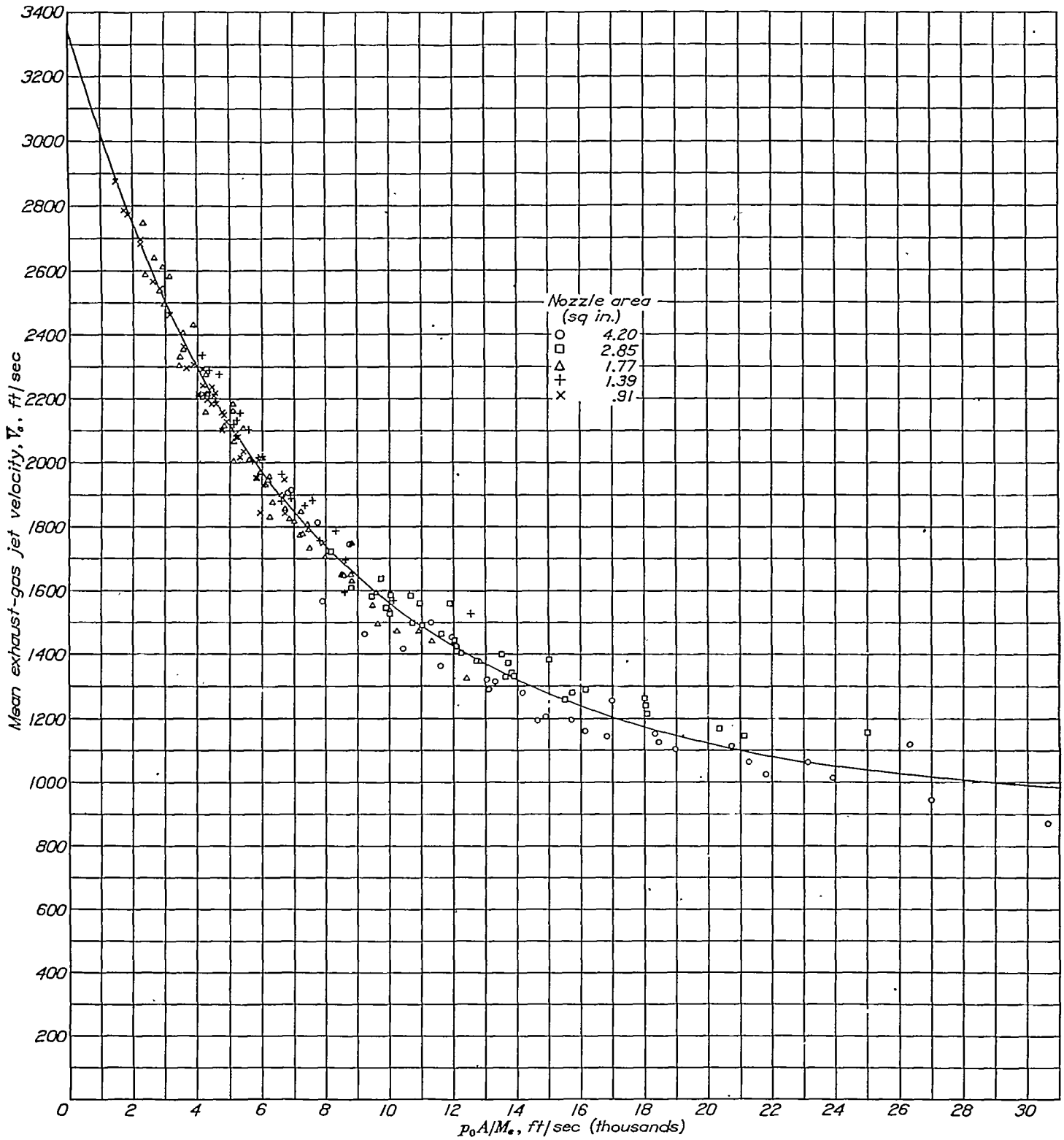

FIGURE 18.—Correlation of all data on variation of mean exhaust-gas jet velocity $\bar{V}_e$ with p_0A/M_e for 25-inch stack.

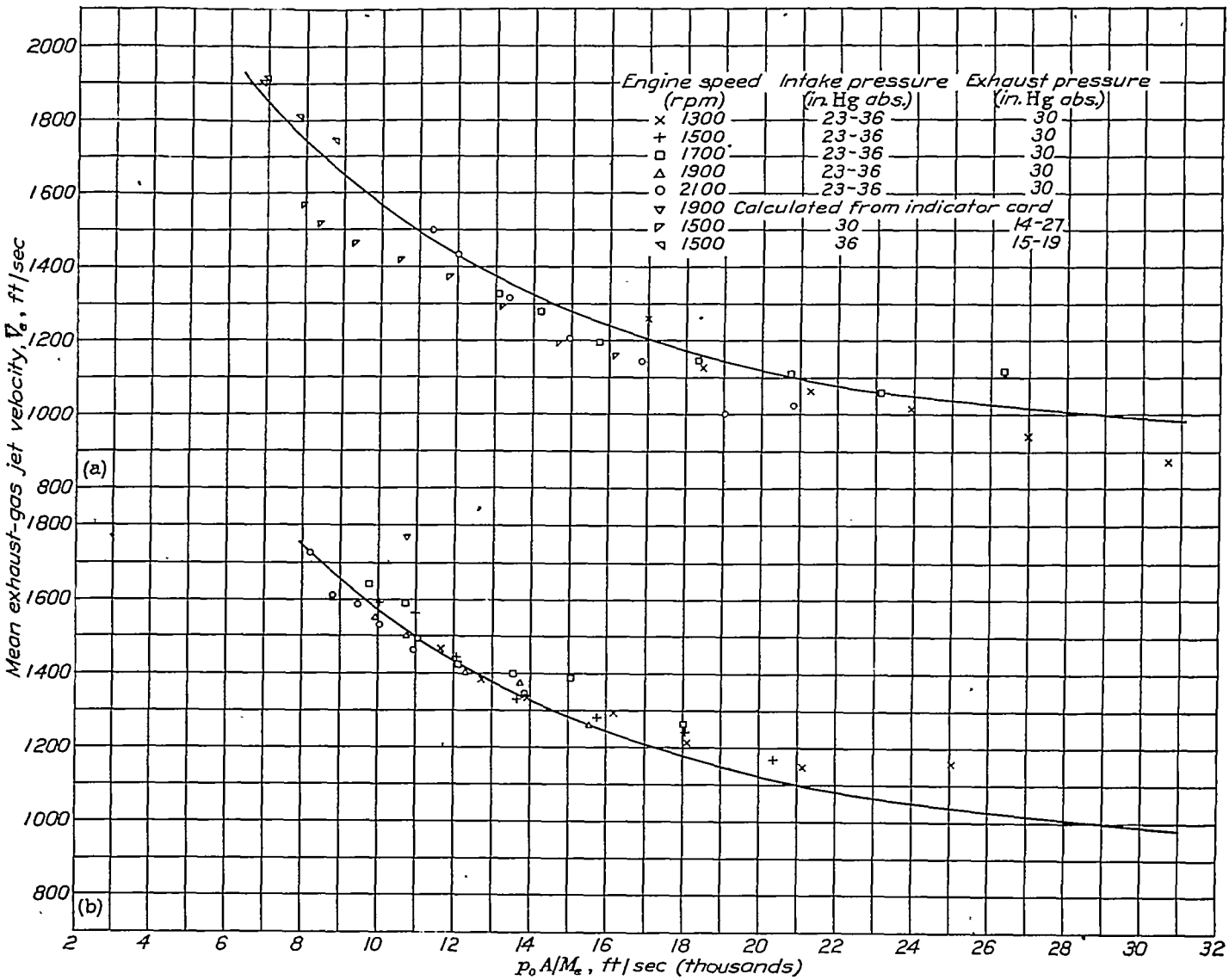

(a) Nozzle area, 4.20 square inches. (b) Nozzle area, 2.85 square inches.

FIGURE 19.—Variation of mean exhaust-gas jet velocity $\overline{V}_e$ with $p_0 A/M_e$ for 25-inch stack.

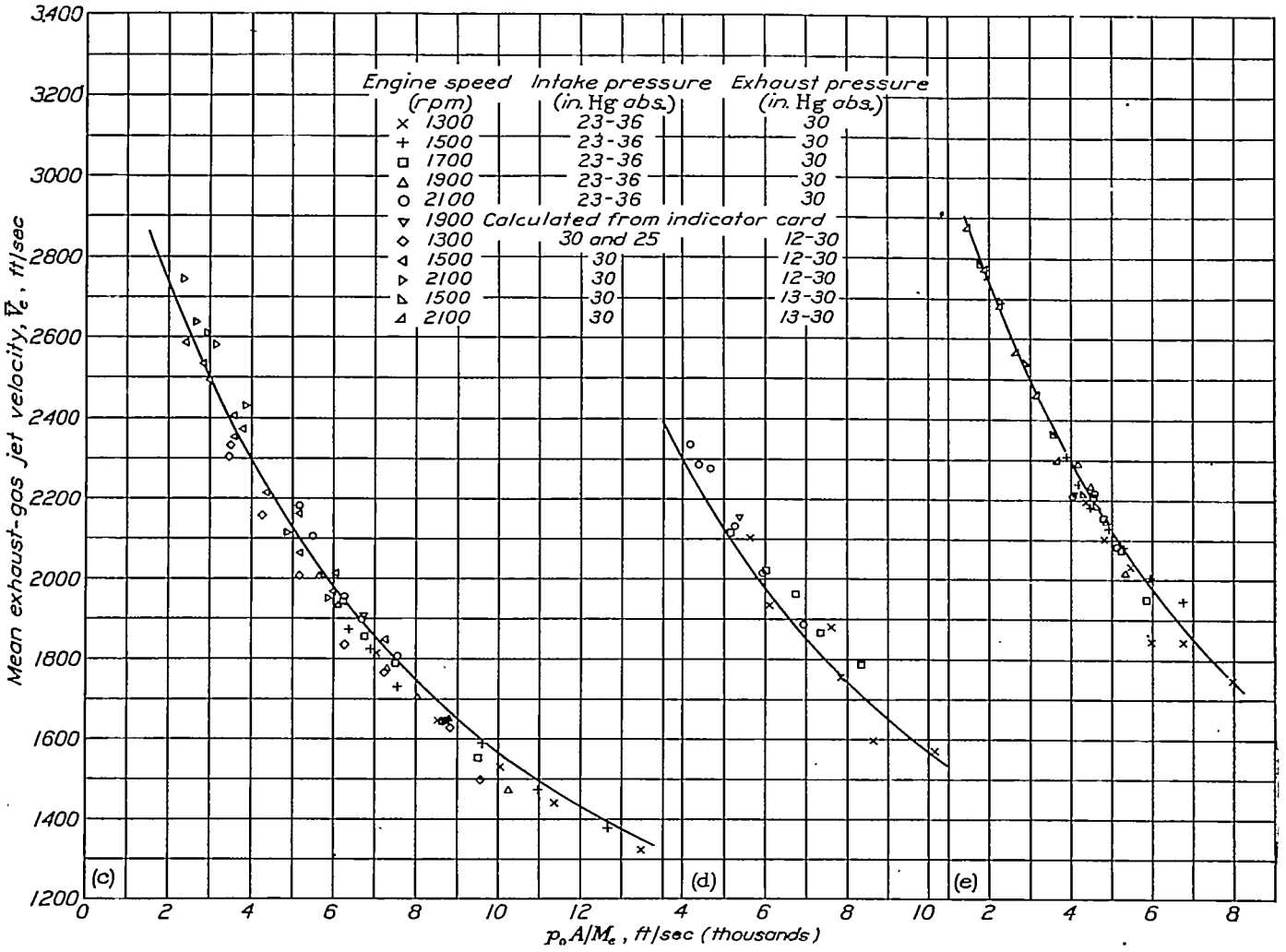

(c) Nozzle area, 1.77 square inches. (d) Nozzle area, 1.39 square inches. (e) Nozzle area, 0.91 square inch

FIGURE 19.—Concluded. Variation of mean exhaust-gas jet velocity $\overline{V}_e$ with $p_o A/M_e$ for 25-inch stack.

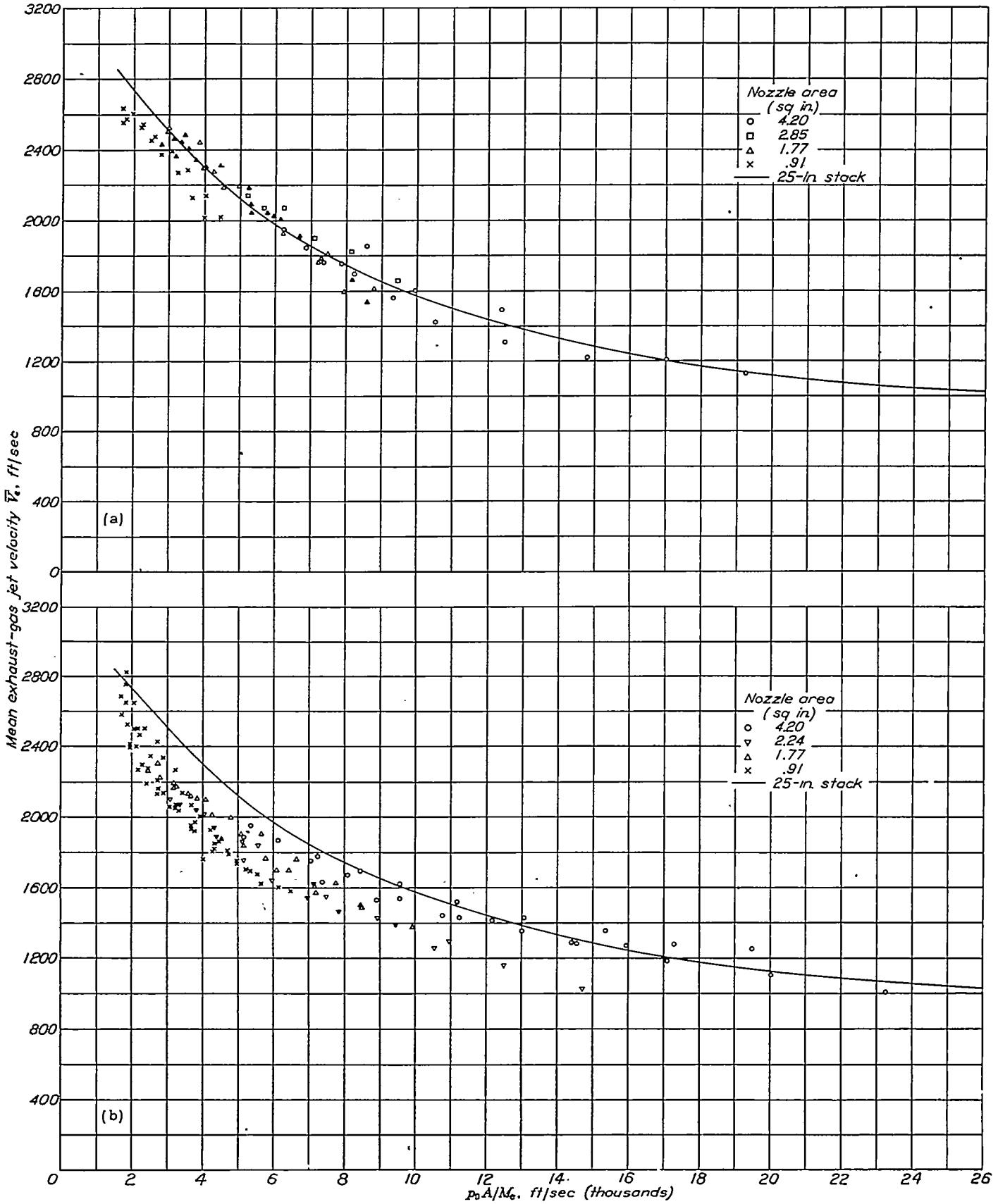

(a) 180° bend
(b) Branched stack.

FIGURE 20.—Variation of $\overline{V}_e$ with p_0A/M_e.

These data were intended to show the effect of discharging into a common stack the exhaust from two cylinders firing alternatively as in a multicylinder installation. Because of the complexity of the phenomenon in branched stacks, doubt exists as to the general applicability of these data.

The static pressures in the cylinder and the exhaust stacks measured by means of the Farnboro indicator are shown in figure 21 for a series of nozzle sizes and the 25-inch stack at the following engine conditions:

Engine speed, rpm	1900
Inlet-manifold pressure, in. Hg	30
Atmospheric pressure, in. Hg	30
Fuel-air ratio	0.08

The impact pressure in the exhaust stack, calculated by means of equations developed in appendix II of reference 3, is also shown in this figure. The impact pressure for the large nozzles is considerably less than the cylinder pressure, showing a large loss in available mechanical energy through the exhaust port. As the nozzle size is decreased, the impact pressure in the stack approaches the cylinder pressure and the loss in available mechanical energy is decreased. The increase in available mechanical energy results in an increase in exhaust thrust. The values of the exhaust thrust, calculated from the impact pressures and those computed from the faired curve in figure 18, are given in the key of figure 21 and are seen to be in fair agreement.

The engine power also was measured while the indicator cards were taken. At this time the exhaust stack was open to the atmosphere; the values of ϕ thus serve to check the values determined when the stack discharged into a closed tank. The values of ϕ shown in figure 21 remain substantially constant until a nozzle area between 2.24 and 1.77 square inches is reached, beyond which further reduction in nozzle area causes a large decrease in power. The results obtained with the exhaust tank show that the maximum value of $v_d n/A$ for no loss in engine power for $p_o/p_m=1$ is 250 feet per second. This value of $v_d n/A$ lies between the values for the 2.24- and 1.77-square-inch nozzles and thus checks the results obtained with atmospheric exhaust.

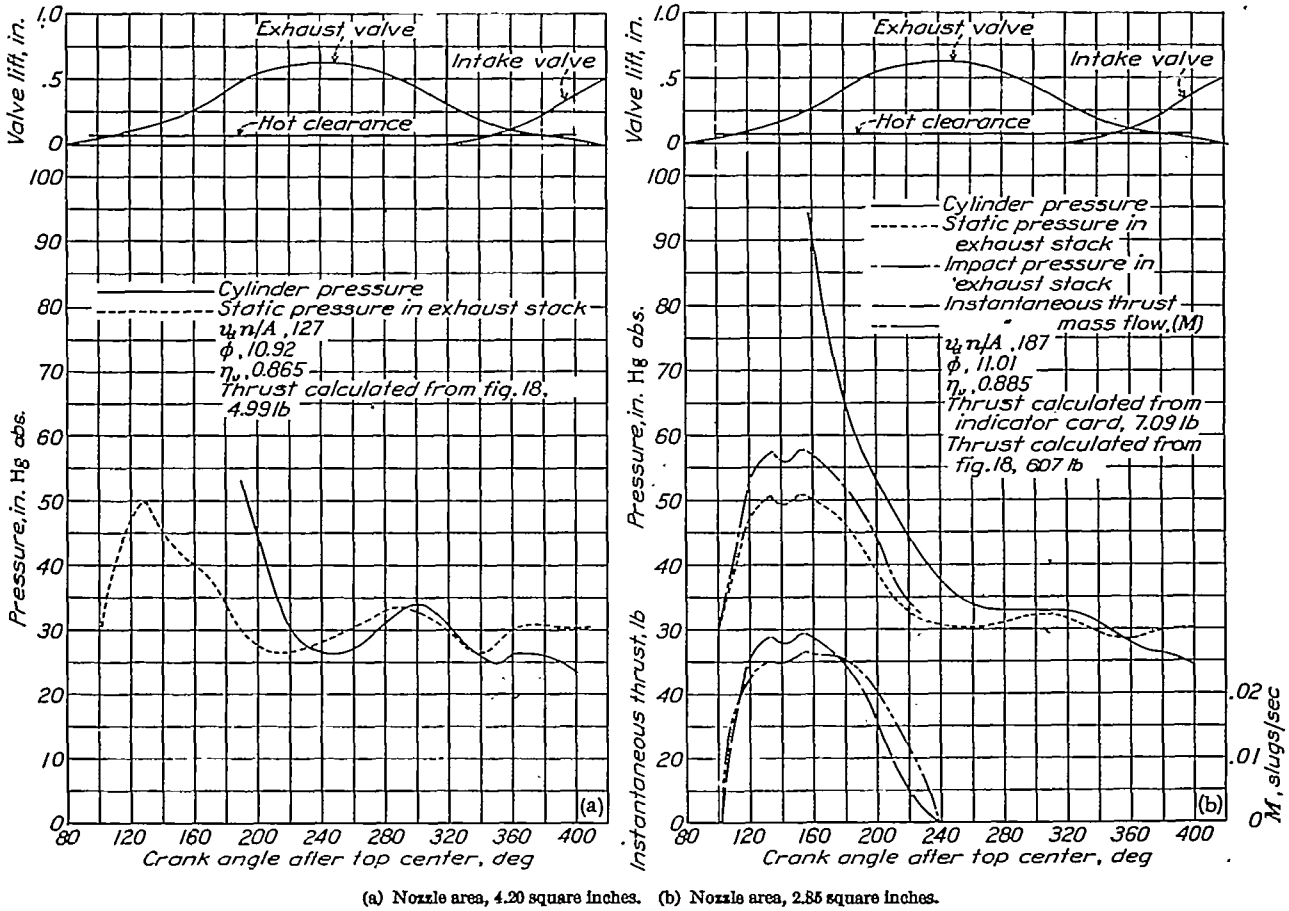

(a) Nozzle area, 4.20 square inches. (b) Nozzle area, 2.85 square inches.

FIGURE 21.—Effect of nozzle area on pressure-time diagram in cylinder and exhaust stack and on rate of exhaust discharge. Engine speed, 1900 rpm; sea-level exhaust and inlet-manifold pressures; fuel-air ratio, 0.08; 25-inch stack.

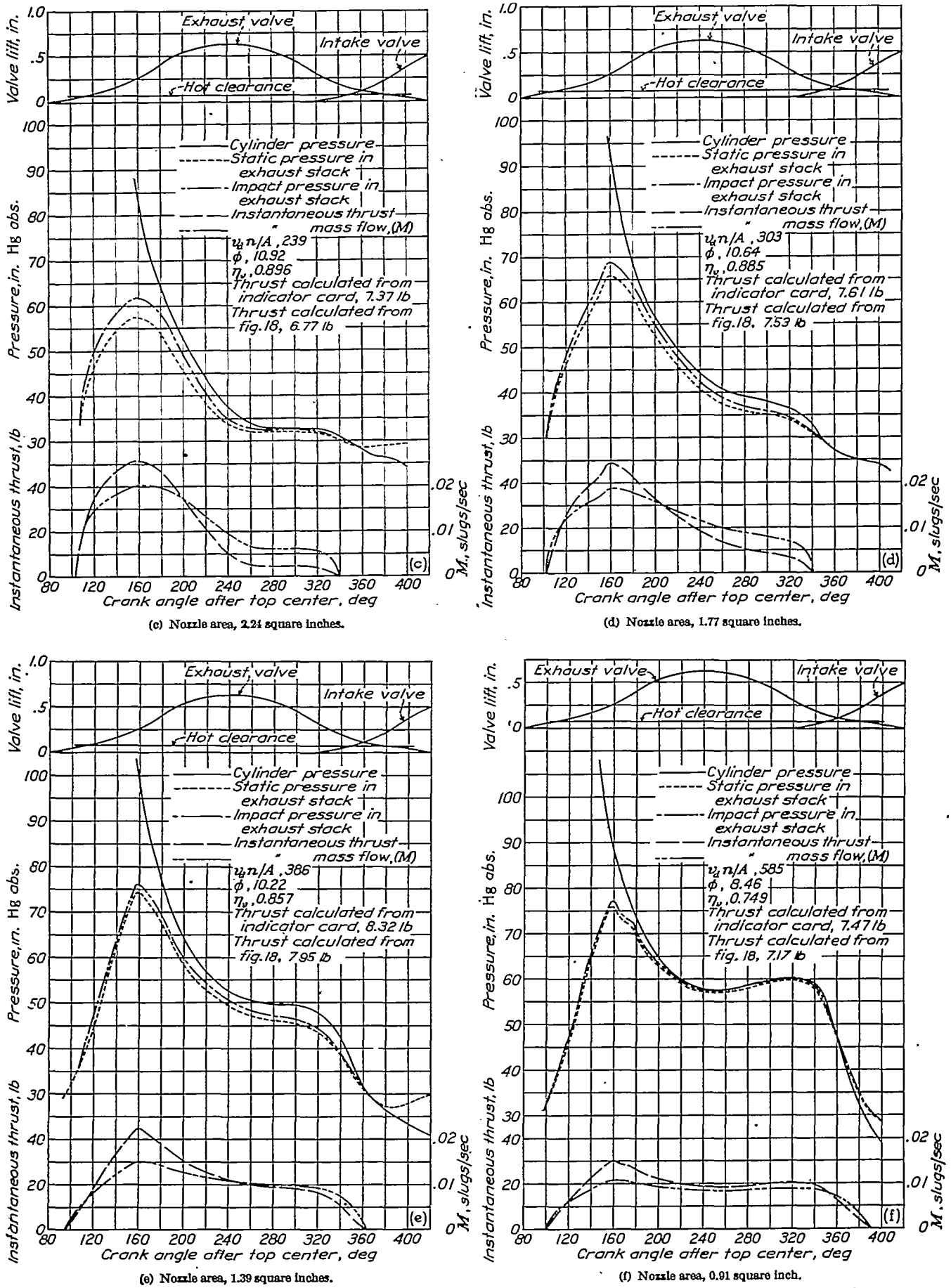

(c) Nozzle area, 2.24 square inches.

(d) Nozzle area, 1.77 square inches.

(e) Nozzle area, 1.39 square inches.

(f) Nozzle area, 0.91 square inch.

FIGURE 21.—Concluded. Effect of nozzle area on pressure-time diagram in cylinder and exhaust stack and on rate of exhaust discharge. Engine speed, 1,900 rpm; sea-level exhaust and inlet-manifold pressures; fuel-air ratio, 0.08; 25-inch stack.

EFFECT OF NOZZLE AREA AND STACK SHAPE ON NET THRUST

Values of effective mean exhaust-gas velocity, $(\overline{V}_e)_{eff}$ as determined by equation (5) are shown in figure 22 plotted against $p_o A/M_e$ at constant values of p_o/p_m for three values of airplane velocity divided by propeller efficiency V/η_p. Curves are given for the 25-inch stack, the S-shaped stack, and the 90° bend. These curves were computed on the basis of $T_m=540°$ R, $f=0.08$, and η_v at 2100 rpm. Volumetric efficiency was determined by the relation

$$\eta_v=\eta_{v,o}+\Delta\eta_v$$

where $\eta_{v,o}$ was the value at 2100 rpm and $\Delta\eta_v$ was obtained from the appropriate curves of $\Delta\eta_v$ against $v_d n/A$. Values of $\Delta\phi$ were obtained from faired curves of $\Delta\phi$ against $v_d n/A$ and $\overline{V}_e$ was obtained from the curves of $\overline{V}_e$ against $p_o A/M_e$ for the 25-inch stack.

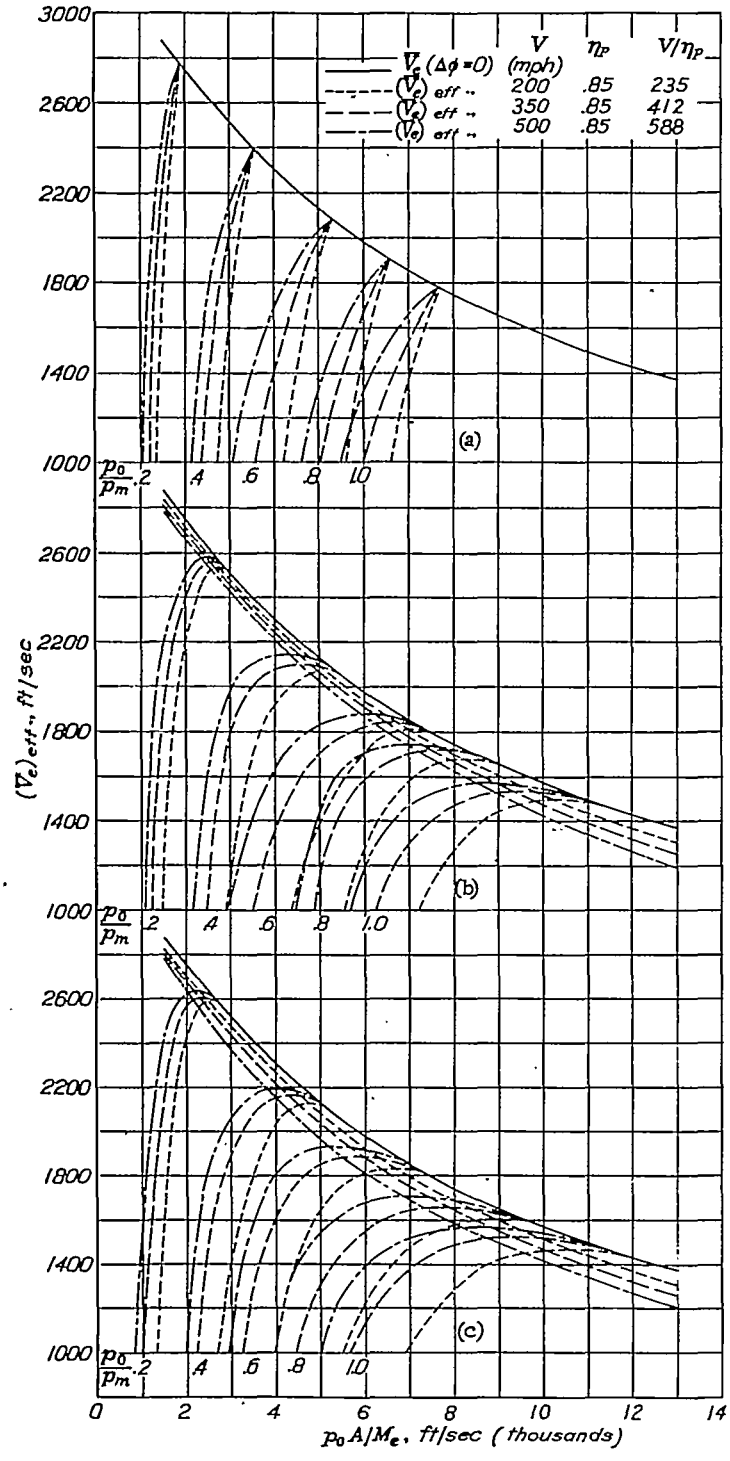

(a) 25-inch stack.
(b) S-shaped stack.
(c) 90° bend.

FIGURE 22.—Variation of $(\overline{V}_e)_{eff}$ with $p_o A/M_e$.

As $p_o A/M_e$ is reduced (at constant p_o/p_m) by reducing the area A, $(\overline{V}_e)_{eff}$ continuously increases until the point is reached at which the engine begins to lose power. At this point $(\overline{V}_e)_{eff}$ branches from the curve for $\overline{V}_e$ ($\Delta\phi=0$) and eventually falls toward zero. For the 25-inch stack the maximum value of $(\overline{V}_e)_{eff}$ occurs at the point where the engine first loses power independently of airplane speed because the loss in engine power occurs abruptly. For the curved stacks the incidence of loss in engine power is gradual; hence, for each airplane speed, $(\overline{V}_e)_{eff}$ continues to increase until the optimum nozzle areas for that speed is reached; thereafter $(\overline{V}_e)_{eff}$ decreases. Lines showing the maximum value of $(\overline{V}_e)_{eff}$ for airplane speeds of 200, 350, and 500 miles per hour have been drawn in figures 22 (b) and 22 (c).

It is noted that these maximum values of $(\overline{V}_e)_{eff}$ in figures 22 (b) and 22 (c) are obtained only at the optimum value of $v_d n/A$ for each value of p_o/p_m and V/η_p. The relative values of the maximum values of $(\overline{V}_e)_{eff}$ for different airplane speeds at constant $p_o A/M_e$ have no significant meaning because for constant values of p_o/p_m the maximums occur at different values of $p_o A/M_e$ for each airplane speed.

It is noted that for the curved stacks (figs. 22 (b) and 22 (c)) the curves of $(\overline{V}_e)_{eff}$ against $p_o A/M_e$ for constant p_o/p_m are relatively flat near their maximum values and the nozzle area may vary considerably without greatly affecting the net gain in thrust power.

The optimum values of $v_d n/A$ plotted against p_o/p_m for the S-shaped stack and the 90° bend are shown in figure 23. The optimum values of $v_d n/A$ are the values for which the gain in net thrust horsepower is a maximum at the given values of p_o/p_m and V/η_p. Optimum values for the 25-inch stack, which are the same as the critical values when $\Delta\phi=0$ (fig. 17), are superimposed on the curves for the two curved stacks. These optimum values were calculated from equation (6) using the values of p_o/p_m and $p_o A/M_e$ for maximum $(\overline{V}_e)_{eff}$ corresponding to $\Delta\phi=0$ and to values of V from 200 to 500 miles per hour (fig. 22).

Inspection of figure 23 shows that the optimum value of $v_d n/A$, for a constant value of p_o/p_m, increases with V; thus, for a given engine and engine speed, the correct nozzle area will decrease as V increases. The optimum values of $v_d n/A$ decreases as the ratio p_o/p_m decreases indicating that, in general, the required nozzle area will increase with the critical altitude. The optimum values of $v_d n/A$ for the S-shaped stack and for the 90° bend are substantially the same.

Figure 23 is convenient for determining the correct nozzle area for a given set of conditions. Figure 22 can be used to predict the gain in performance to be expected from the installation.

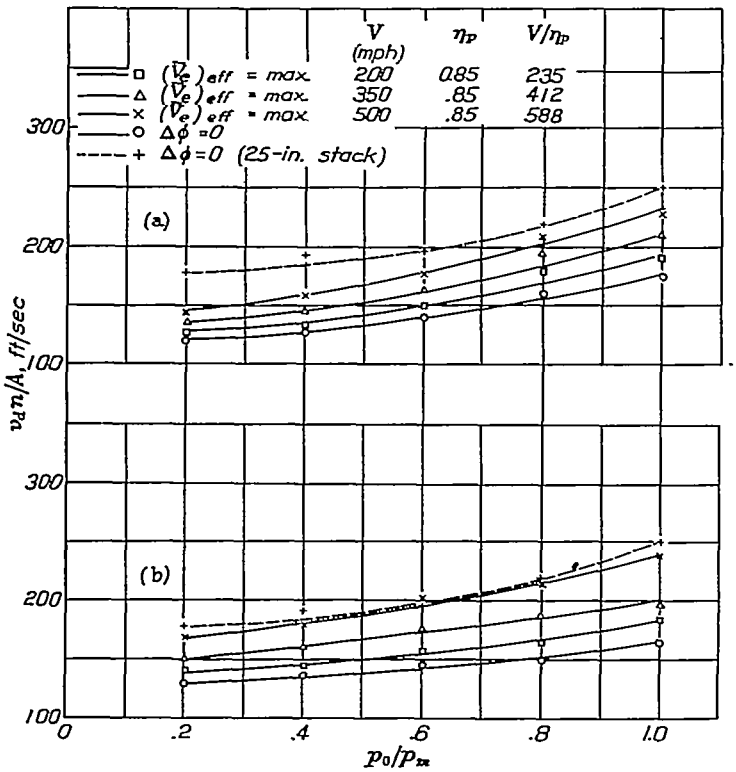

(a) S-shaped stack.
(b) 90° bend.

FIGURE 23.—Variation of optimum values of $v_d n/A$ with p_o/p_m.

The method of using the curves is shown by the following example if the following conditions are assumed:

Engine displacement volume, cu in.	1800
Number of cylinders	14
Engine speed, rpm	2400
Brake horsepower	1100
Atmospheric pressure, in. Hg absolute	13.75
Inlet-manifold pressure, in. Hg absolute	43.00
Propeller efficiency	0.85
Airplane velocity, mph	350

Then $p_o/p_m=13.75/43.0=0.32$

If S-shaped stacks are used, the value of $v_d n/A$ corresponding to maximum performance is 145 (fig. 23(a)). The nozzle area per cylinder is given by

$$\text{area}=\frac{v_d n}{145}=\frac{1800}{14\times 1728}\times\frac{2400}{60}\times\frac{144}{145}=2.96 \text{ square inches}$$

For a charge consumption of 2.4 pounds per second $p_o A/M_e$ is given by

$$\frac{p_o A}{M_e}=13.75\times 0.491\times 144\times\frac{2.96}{144}\times\frac{14\times 32.2}{2.4}$$

$$=3750 \text{ feet per second}$$

From figure 22(b) the corresponding value of $(\overline{V}_e)_{eff}$ is 2300 feet per second and the net gain in thrust horsepower is given by

$$\Delta P_T=\frac{M_e(\overline{V}_e)_{eff}V}{550}=\frac{2.4}{32.2}\times\frac{2300}{550}\times 514=160.0 \text{ horsepower}$$

This value is 17.12 percent of the engine thrust horsepower. On the assumption that the airplane velocity varies as the cube root of the thrust horsepower, the increase in V is given by

$$\Delta V=350[\sqrt[3]{1.1712}-1]=18.9 \text{ miles per hour}$$

The thrust horsepower of the jet alone is obtained using $\overline{V}_e$ from the curve $\Delta\phi=0$ and is equal to P_J where

$$P_J=\frac{M_e\overline{V}_e V}{550}=\frac{2.4}{32.2}\times\frac{2350}{550}\times 514=163.5 \text{ horsepower}$$

The difference in thrust horsepower, 163.5—160.0=3.5, is due to the loss in engine power.

If the example is computed on the basis of the value of $v_d n/A$ at which the engine begins to lose power, the required nozzle area is 3.54 square inches per cylinder, which is 19.6 percent greater than the area corresponding to maximum performance. The value of $\overline{V}_e$ for this case becomes 2210 feet per second, P_J becomes 154.3 horsepower, and the value of ΔV is approximately 18.2 miles per hour. The difference in performance with the two nozzle areas is slight and the use of the large nozzle is probably better from consideration of engine cooling and the high engine speed required for take-off.

An example of the gain in thrust horsepower to be expected from exhaust-gas jet propulsion is shown in figure 24. In these computations an inlet-manifold temperature of 80°F, an exhaust-gas flow of 0.002 pound per second per brake horsepower, a propeller efficiency of 0.85, and the volumetric efficiency shown for the unrestricted 25-inch stack in figure 9 were assumed. The percentage gain in thrust horsepower

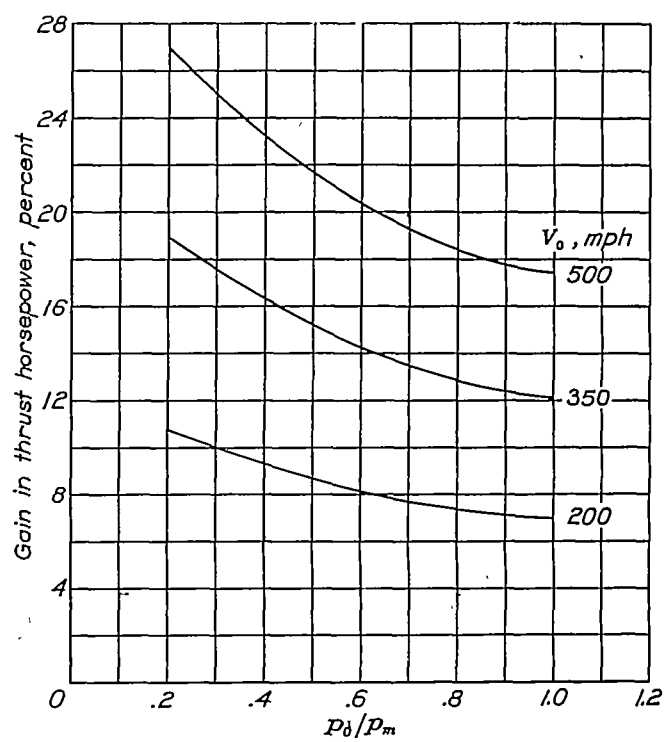

FIGURE 24.—Example of gain in thrust horsepower with exhaust-gas jet propulsion with optimum $v_d n/A$. Exhaust-gas flow, 0.002 pound per second per bhp; η_v, taken from figure 9; η_p, 0.85; 25-inch stack.

at constant airplane velocity V increased at an increasing rate as p_o/p_m decreased; at high airplane velocity (500 mph) and altitude (corresponding to $p_o/p_m=0.2$) the gain in thrust horsepower is 27 percent of the engine thrust horsepower.

The values of $v_d n/A$ used in the preceding examples to determine the optimum nozzle area are smaller than the corresponding values of $v_d n/A$ at which the air flow to the engine begins to fall off. Consequently, the percentage increase in thermal efficiency will be the same as the gain in thrust horsepower.

CONCLUSIONS

Based on test-stand measurements of the effect of exhaust-stack-nozzle area, shape, and length on engine power and exhaust-gas thrust for an 1820-G single-cylinder engine operating from 1300 to 2100 rpm, inlet-manifold pressure from 24 to 36 inches mercury absolute, and simulated altitude pressure from 12 to 30 inches mercury absolute, it is concluded that:

1. The variation of engine power with exhaust-stack-nozzle area may be correlated in terms of two variables; (a) the ratio of simulated altitude pressure to the inlet-manifold pressure and (b) the product of the engine displacement volume and the engine speed divided by the nozzle area.

2. For each stack and engine operating condition, a critical nozzle area exists below which a loss in engine power occurs.

3. The presence of smooth bends in individual exhaust stacks having no nozzle restriction had no appreciable effect on engine power.

4. Increases of stack length up to 44 inches had no effect on engine power; a stack 108 inches long had an adverse effect on engine power for most practical combinations of nozzle area and engine speed.

5. The data on exhaust-gas thrust may be correlated by plotting the mean exhaust-gas jet velocity against the product of the atmospheric pressure and the nozzle area divided by the mass of exhaust gas discharge per unit time.

6. The mean exhaust-gas jet velocity obtained with individual exhaust stacks was not appreciably changed by the addition of smooth bends to the exhaust stack or by changes in length up to at least 44 inches. The curve obtained for the 25-inch stack may be used to predict the thrust obtainable with stacks in the foregoing classification.

7. Large gains in net thrust can be obtained by use of jet stacks. This thrust power is proportional to airplane speed and at 500 miles per hour at a ratio of altitude pressure to inlet-manifold pressure of 0.2, the jet-thrust power is 27 percent of the engine thrust horsepower.

LANGLEY MEMORIAL AERONAUTICAL LABORATORY,
NATIONAL ADVISORY COMMITTEE FOR AERONAUTICS,
LANGLEY FIELD, VA., *August 14, 1942.*

REFERENCES

1. Oestrich, Hermann: Prospects for Jet Propulsion of Airplanes with Special Reference to Exhaust Gases. NACA Misc. Paper No. 34, 1932.
2. Pinkel, Benjamin, and Turner, L. Richard: Flight Tests of Exhaust-Gas Jet Propulsion. NACA ACR, Nov. 1940.
3. Pinkel, Benjamin, Turner, L. Richard, and Voss, Fred: Design of Nozzles for the Individual Cylinder Exhaust Jet Propulsion System. NACA ACR, April 1941.
4. Turner, L. Richard, and Humble, Leroy V.: The Effect of Exhaust-Stack Shape on the Design and Performance of the Individual Cylinder Exhaust-Gas Jet-Propulsion System. NACA ARR, Nov. 1942.